RSC Advances

PAPER

View Article Online
View Journal | View Issue

Check for updates

Cite this: *RSC Adv.*, 2021, **11**, 37684

C(acyl)–C(sp^2) and C(sp^2)–C(sp^2) Suzuki–Miyaura cross-coupling reactions using nitrile-functionalized NHC palladium complexes†

Sinem Çakır, [a] Serdar Batıkan Kavukcu, [a] Hande Karabıyık,[b] Senthil Rethinam[cd] and Hayati Türkmen *[a]

Received 28th September 2021
Accepted 8th November 2021

DOI: 10.1039/d1ra07231e

rsc.li/rsc-advances

Application of N-heterocyclic carbene (NHC) palladium complexes has been successful for the modulation of C–C coupling reactions. For this purpose, a series of azolium salts (**1a–f**) including benzothiazolium, benzimidazolium, and imidazolium, bearing a CN-substituted benzyl moiety, and their $(NHC)_2PdBr_2$ (**2a–c**) and PEPPSI-type palladium (**3b–f**) complexes have been systematically prepared to catalyse acylative Suzuki–Miyaura coupling reaction of acyl chlorides with arylboronic acids to form benzophenone derivatives in the presence of potassium carbonate as a base and to catalyse the traditional Suzuki–Miyaura coupling reaction of bromobenzene with arylboronic acids to form biaryls. All the synthesized compounds were fully characterized by Fourier Transform Infrared (FTIR), and ^{1}H and ^{13}C NMR spectroscopies. X-ray diffraction studies on single crystals of **3c**, **3e** and **3f** prove the square planar geometry. Scanning Electron Microscopy (SEM), energy dispersive X-ray spectroscopy (EDS), metal mapping analyses and thermal gravimetric analysis (TGA) were performed to get further insights into the mechanism of the Suzuki–Miyaura cross coupling reactions. Mechanistic studies have revealed that the stability and coordination of the complexes by the CN group are achieved by the removal of pyridine from the complex in catalytic cycles. The presence of the CN group in the (NHC)Pd complexes significantly increased the catalytic activities for both reactions.

Open Access Article. Published on 23 November 2021. Downloaded on 9/22/2024 3:55:22 AM.
This article is licensed under a Creative Commons Attribution-NonCommercial 3.0 Unported Licence.

Introduction

The modification of organic compounds such as natural compounds, pharmaceuticals, and novel materials can be achieved through the formation of carbon–carbon bonds. Carbon–carbon bond formation is the most useful transformation for chemists in the preparation of organic compounds.[1] Palladium-catalyzed coupling reactions of aryl, alkyl halides or acyl chlorides with organoborons are the easiest and safest way to access C(sp^2)–C(sp^2) or C(acyl)–C(sp^2) bonds and to prepare biaryls or ketones.[2] Many synthetic methods have been developed for the synthesis of ketones in general due to their formation in various natural products, agrochemicals, fine chemicals, and pharmaceutical products.[3] The palladium-catalyzed acylative Suzuki–Miyaura cross coupling reaction has gained great attention due to its easy accessibility, and use of widely functionalized, partially low toxicity, heat and moisture resistance of organoborons. Besides, this method can prevent the restrictions of the regioselectivity limitation, the requirement of the directional group (carbonylative), the use of the *para* position (conventional Friedel–Crafts acylation), the use of toxic carbon monoxide, and the formation of biaryl by-products (carboxylative Suzuki–Miyaura cross-coupling), CH activation conditions (oxidation of benzyl alcohols and addition of organometallic reagents to carboxylic derivatives or nitriles), and incompatibility with electron-deficient groups.[4] Due to these advantages, recently, palladium-mediated cross-coupling reactions between arylboronic acid and an activated derivative of an acyl chloride has been reported to be effective in synthesizing functionalized ketones.[5]

The palladium-catalyzed traditional Suzuki–Miyaura cross-coupling reaction of organoboron reagents with aryl halides to form biaryl derivatives has emerged over the past two decades as an extremely powerful tool in organic synthesis.[3c-d] The reaction conditions for Suzuki–Miyaura couplings involve the use of homogeneous palladium catalysts containing phosphine ligands[7] or N-heterocyclic carbene (NHC) ligands.[6] The first NHC was discovered by Wanzlick *et al.* in 1968, and in 1991, it was isolated and structure determined by Arduengo *et al.*[8] Carbenes from many NHC ligands containing other donor functions (such as imidazole, benzimidazole, imidazoline, and

[a]*Department of Chemistry, Ege University, 35100 Bornova, Izmir, Turkey. E-mail: hayatiturkmen@hotmail.com*

[b]*Department of Physics, Faculty of Science and Art, Dokuz Eylül University, Izmir, Turkey*

[c]*School of Natural and Applied Science, Ege University, Bornova, Izmir, 35100, Turkey*

[d]*School of Bio & Chemical Engineering, Sathyabama University, Chennai, 600 199, Tamilnadu, India*

† Electronic supplementary information (ESI) available. CCDC 2071690, 2071692 and 2071693. For ESI and crystallographic data in CIF or other electronic format see DOI: 10.1039/d1ra07231e

© 2021 The Author(s). Published by the Royal Society of Chemistry

Open Access Article. Published on 23 November 2021. Downloaded on 9/22/2024 3:55:22 AM.
This article is licensed under a Creative Commons Attribution-NonCommercial 3.0 Unported Licence.

1,2,4-triazole) can affect metal complexes with enhanced stability and catalytic activity.[9] On the other hand, heterobidentate ligands are hybrid ligands that combine the properties of two different donor atoms. These ligands affect the equilibrium because both the metal ion and the chelating agent are sensitive to changes in the catalytic system. Pd complexes with hybrid NHC ligands (with S–C, O–C, N–C, or P–C coordination mode) are well known as generally good catalysts for C–C bond formation reactions.[10] They control metal ions by blocking the reactive sites of the metal ion and preventing them from entering into their normal (and in many cases undesirable) reactions. As coordination flexibility in hybrid ligands can have a profound effect on catalytic performance,[11] we were interested in effect of NHC structure and nitrile group on catalytic activities. So, the azolium salts (benzothiazolium, benzimidazolium, imidazolium) containing 2-nitrile substituted benzyl groups and not nitrile group were prepared. Their palladium(II) complexes were synthesized and their catalytic activities were also tested in the direct arylation of acyl chlorides and Suzuki–Miyaura coupling reaction. The catalytic activities of the palladium(II) complexes varied with different NHC skeletons which is the most important way to modify.

This study primarily focused on the acylative Suzuki–Miyaura cross-coupling reaction. The different strategies for the acylative Suzuki–Miyaura cross-coupling reaction of benzoyl chloride with phenylboronic acid are illustrated in Fig. 1. In early works, Bumagin *et al.* and Haddach *et al.* evolved palladium-catalyzed cross-coupling of arylboronic acids with acyl chlorides in 1999.[12a,b] Li *et al.* developed an imidazolium chloride tagged Pd(II) complex for the reaction but high catalyst loading and long reaction time was needed.[12c] Bora *et al.* reported two different procedure and one was required high catalyst loading,[12d] while the other one was reached 97% yield in 4 hours with 0.4 mol% catalyst.[12h] Štěpnička *et al.* published immobilized palladium catalysts[12f] and Pd(II) complex with phosphinoferrocene ligands bearing extended polar amidourea pendants[12e] for the acylative Suzuki–Miyaura coupling reaction. They reached 618 TON value with the Pd(II) complex with phosphinoferrocene ligand. Rafiee *et al.* developed catalytic system using 1-benzyl-4-aza-1-azoniabicyclo[2.2.2]octane chloride and $PdCl_2$.[12g] Movassagh *et al.* reported polystyrene-supported NHC–Pd(II) complex and their heterogeneous catalyst could be reused up to four times.[12i] In this context, we have prepared nitrile-functionalized NHC precursors and their Pd(II) complexes as a precatalysts to investigate whether $(NHC)_2PdBr_2$ and PEPPSI type Pd complexes would be also useful for the acylative Suzuki–Miyaura cross-coupling reaction of acyl chlorides with phenylboronic acids to give biaryl ketones. Also, the performance of the Pd(II) complexes in the traditional Suzuki–Miyaura cross-coupling reaction was evaluated. Both reactions were carried out under mild conditions.

Results and discussion

Synthesis of the azolium salts and Pd(II) complexes

Electronic σ-donor properties of NHCs are significantly affected by the presense of the heterocyclic skeleton.[13] The most preferred heterocyclic skeletons in catalyst chemistry are imidazole, benzimidazole and benzothiazole. To understand the effect of heterocyclic skeleton structure (benzothiazole,

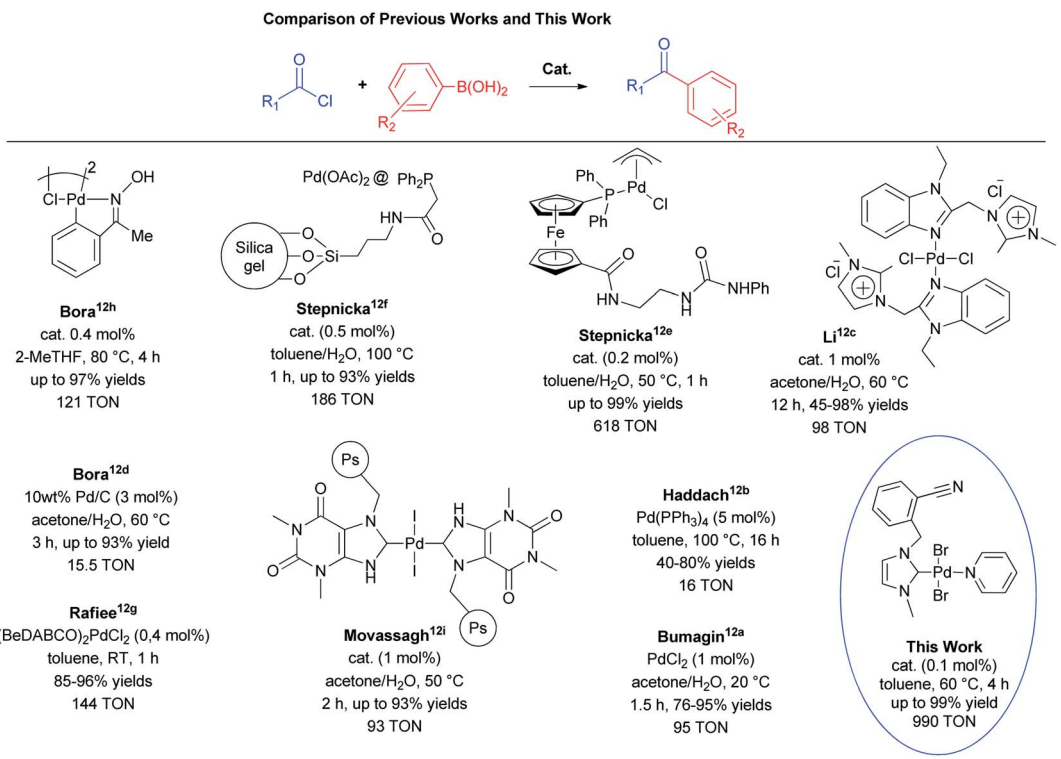

Fig. 1 Strategies for the acylative Suzuki–Miyaura cross coupling reaction.

Open Access Article. Published on 23 November 2021. Downloaded on 9/22/2024 3:55:22 AM.
This article is licensed under a Creative Commons Attribution-NonCommercial 3.0 Unported Licence.

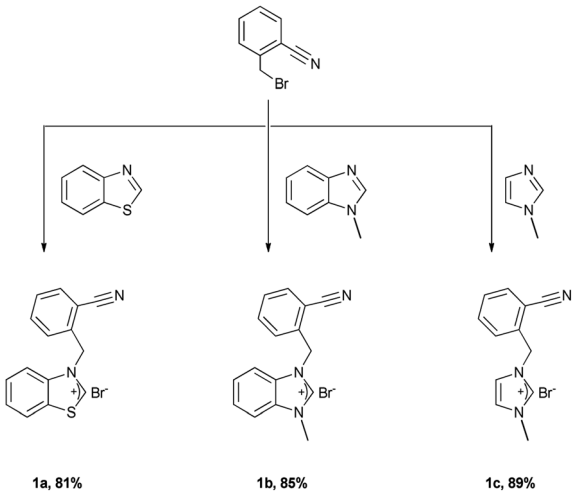

Scheme 1 Synthesis route to the NHC precursors **1a–c**.

benzimidazole, and imidazole) on Pd(II) complex in the Suzuki–Miyaura cross-coupling reactions, a series of azolium salts bearing 2-nitrile substituted benzyl group and their palladium complexes were prepared. The azolium salts **1a–c** were prepared in one-pot reaction consisting of the alkylation of benzothiazole, 1-methyl-benzimidazole and 1-methyl-imidazole, by 2-(bromomethyl)benzonitrile in toluene for 24 h (Scheme 1). The new azolium salts (**1a–c**) were obtained as white solids in 81, 85, 89% yields, respectively and they displayed good solubility in

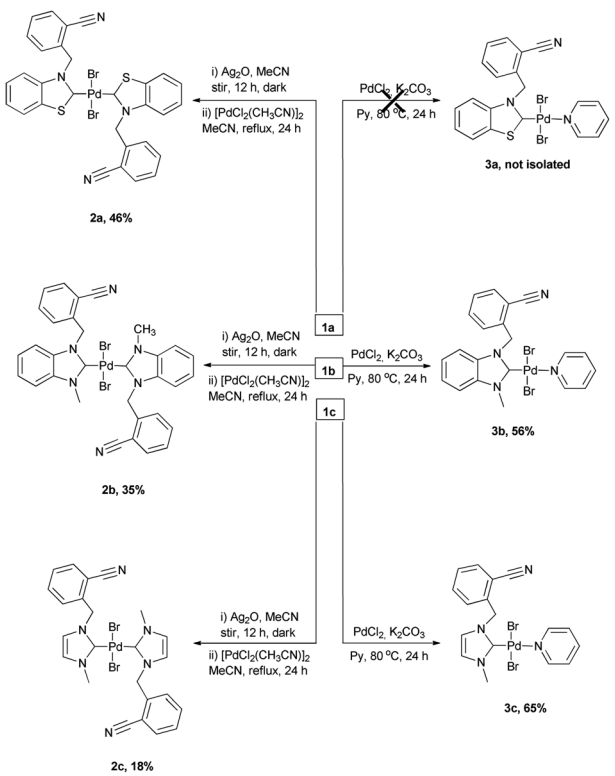

Scheme 2 Synthesis route to the NHC–Pd(II) complexes **2a–c** and **3a–c**.

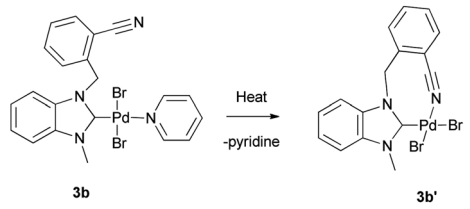

Scheme 3 Preparation of the NHC–Pd(II) chelate complex **3b′**.

polar solvents. They were characterized by ^{1}H and ^{13}C NMR spectroscopy. The NMR spectrums of **1a–c** were agreed with the proposed structures: C2–H resonance at $\delta = 10.80$–9.33 ppm as a sharp singlet in the ^{1}H NMR spectrums and these downfield signals demonstrate the formation of azolium salts. Also, the chemical shift of C≡N sp hybrid carbon atoms of **1a–c** were detected in the ^{13}C NMR spectrums at δ 117.5, 117.4, and 117.0 ppm, respectively. The synthesis route to Pd(II) complexes (**2a–c**, **3a–c**) were summarized in Scheme 2. The new $(NHC)_2$-$PdBr_2$ complexes (**2a–c**) were synthesized in two-step sequence consisting of the transmetalation from the *in situ* formed NHC–Ag species.[14] The PEPPSI type Pd(II) complexes **3b**, **3c** were obtained deprotonation of **1b**, **1c** with K_2CO_3 in pyridine, respectively. Unfortunately, **3a** could not be isolated. The chelate complex **3b′** was obtained by heating of **3b** to remove the pyridine ligand (Scheme 3). To understand the important of the position, the number of CN, and the absence of CN on NHC–Pd(II) complexes in catalytic activities, imidazolium salts (**1d–f**) were prepared. The complexes (**3d–f**) were prepared according to procedure **3b–c** (Scheme 4). All the novel Pd complexes were obtained in high yields as air- and moisture-stable pale-yellow solids and were characterized by NMR and infrared spectroscopies. In the ^{1}H-NMR spectra of **2a–c**, the CH_2 protons of **2a** demonstrated a singlet peak, whereas the CH_2 protons of **2b** and **2c** exhibited multiplet peaks. This difference in **2b** and **2c** may be due to an intermolecular interaction of hydrogen. The Pd(II) complexes (**3b–f**) displayed characteristic signals Pd–$C_{carbene}$ at $\delta = 164.8$, and 154.3, 152.4, 152.6 and 152.5 ppm,

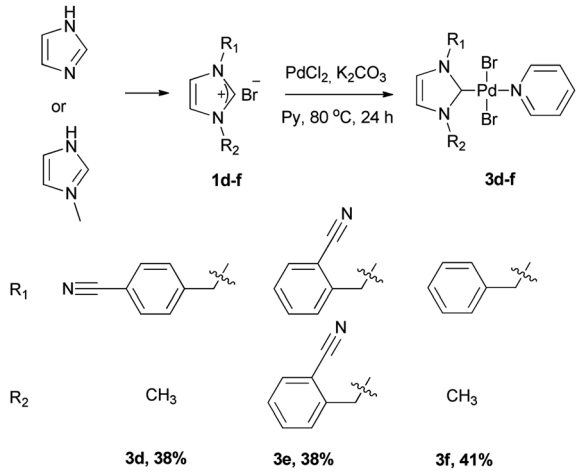

Scheme 4 Synthesis route to the NHC–Pd(II) complexes **3d–f**.

© 2021 The Author(s). Published by the Royal Society of Chemistry

Open Access Article. Published on 23 November 2021. Downloaded on 9/22/2024 3:55:22 AM.
This article is licensed under a Creative Commons Attribution-NonCommercial 3.0 Unported Licence.

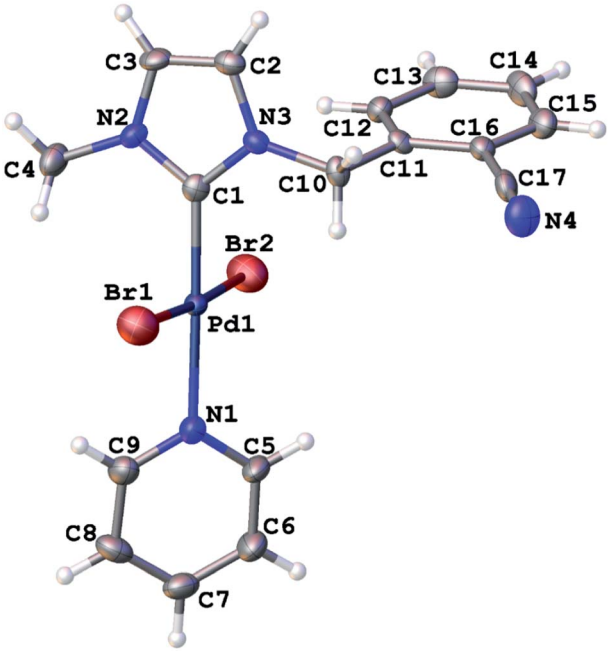

Fig. 2 Molecular structure of complex **3c** with displacements ellipsoids plotted at the 30% probability level. Selected bond lengths (Å) and angles (°): Pd1–C1 1.946(12), Pd1–N1 2.113(10), Pd1–Br1 2.389(2), Pd1–Br2 2.393(2), N2–C1 1.357(14), N3–C1 1.346(15), Br1–Pd1–Br2 175.58(7), C1–Pd1–N1 178.4(5), N1–Pd1–Br1 91.6(3), N1–Pd1–Br2 91.8(3), C1–Pd1–Br1 88.6(3), C1–Pd1– Br2 87.9(3), N3–C1–N2 103.9(1). Dihedral angles: *A*/*B* 86.73(19)°, *A*/*C* 51.97(17)°, *B*/*C* 36.02(15)°.

respectively. The complexes exhibited almost identical FT–IR spectra indicating their similar structure. Due to the tensile vibrations of nitrile functionality (C≡N), a medium-density sharp band was observed at 2221–2227 cm^{-1}. The presence of the –C=N– group in the complexes was verified with the observation of ν(C=N) bands between 1640 and 1539 cm^{-1}.

The crystal and molecular structure of 3c, 3e and 3f complexes

The crystal structures of three similar PEPPSI type Pd(II) complexes **3c**, **3e**, and **3f** were determined using the X-ray single-crystal diffraction technique. Asymmetric unit of **3e** contains a half molecule and the complete molecular structure is generated by the implementation of the crystallographic two-fold rotation whose axis bisects imidazole and pyridine rings as shown in Fig. 3. Asymmetric units of **3c** and **3f** are shown in Fig. 2 and 3, respectively. Selected bond lengths and angles are given in the figure captions for each compound. The coordination plane consisting of Pd, $C_{carbene}$, $N_{pyridine}$ and two Br atoms is slightly distorted from square-planar geometry for all three compounds. These planes are almost planar in **3e** and **3c**. Deviation of $C_{carbene}$ from the mean plane through NHC ring in complex **3f** is −0.109(2) Å. Due to positional disorder, the most prominent deviation from the coordination plane in complex **3f** is observed for Br4A with a value of 0.553(4) Å. Some of Br–Pd–Br and $C_{carbene}$–Pd–$N_{pyridine}$ bond angles are reliably distorted. Deviations from their linearity can be clearly observed for C1–

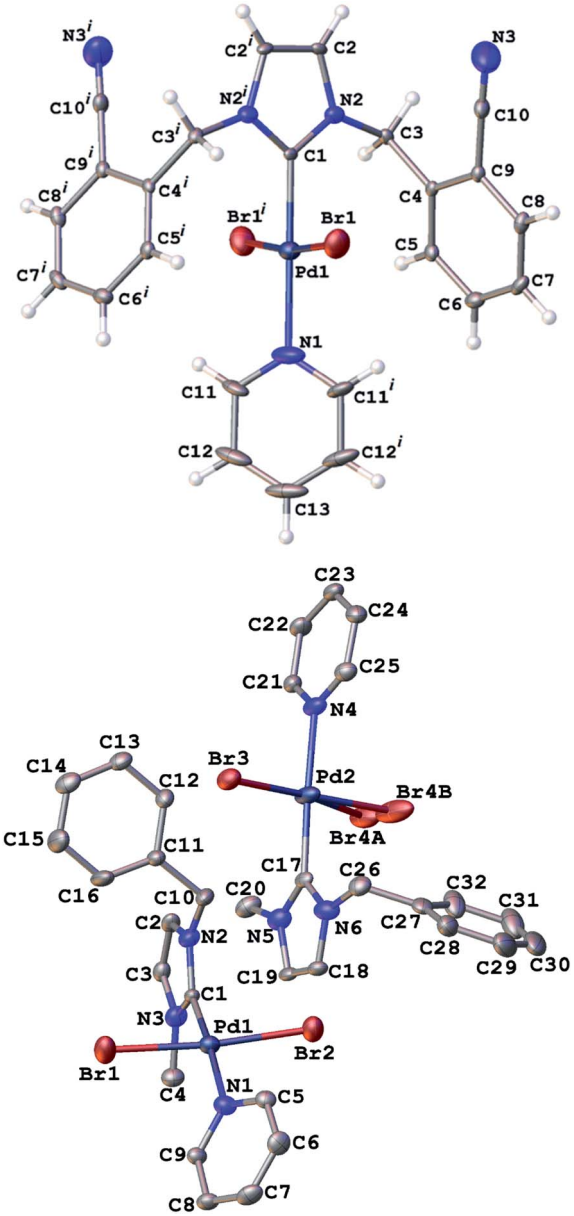

Fig. 3 Molecular structure of **3e** (top) with displacements ellipsoids plotted at the 30% probability level. Symmetry related atoms are labeled with superscript i. Symmetry code: (i) 1 − *x*, *y*, 0.5 − *z*. Selected bond lengths (Å) and angles (°): Pd1–C1 1.946(6), Pd1–N1 2.117(6), Pd1–Br1 2.4465(5), N2–C1 1.342(4), Br1–Pd1–Br1i 172.36(3), C1–Pd1–N1 180.0, C1–Pd1–Br1i 86.18(2), N1–Pd1–Br1 93.82(2), N2–C1–N2i 106.6(5). Dihedral angles: *A*/*B* 76.97(19)°, *A*/*C* 44.5(3)°, *B*/*C* 58.53(19)°. The asymmetric unit of **3f** (bottom) showing the atom-labelling scheme. Hydrogen atoms are omitted for clarity. Displacements ellipsoids are drawn at the 30% probability level. Selected bond lengths (Å) and angles (°): Pd1–C1 1.948(6), Pd2–C17 1.963(6), Pd1–N1 2.090(5), Pd2–N4 2.101(5), Pd1–Br1 2.4265(8), Pd1–Br2 2.4308(8), Pd2–Br3 2.4028(9), Pd2–Br4A 2.490(7), Pd2–Br4B 2.388(3), N3–C1 1.337(7), N2–C1 1.333(6), N5–C17 1.336(7), N6–C17 1.342(7), Br1–Pd1–Br2 174.26(3), C1–Pd1–N1 173.4(2), C17–Pd2–N4 176.0(2), C1–Pd1–Br1 86.72(17), C1–Pd1–Br2 89.51(16), N1–Pd1–Br1 91.60(13), N1–Pd1–Br2 92.63(13), N4–Pd2–Br3 92.78(14), C17–Pd2–Br3 91.13(17), C17–Pd2–Br4B 87.91(18), N4–Pd2–Br4B 88.36(14), N2–C1–N3 105.3(5), N5–C17–N6 104.7(5). Dihedral angles in molecule including Pd1: *A*/*B* 77.07(17)°, *A*/*C* 79.0(2)°, *B*/*C* 10.77(17)°.

Open Access Article. Published on 23 November 2021. Downloaded on 9/22/2024 3:55:22 AM.
This article is licensed under a Creative Commons Attribution-NonCommercial 3.0 Unported Licence.

Pd1–N1 with an angle of 173.4(2)° in **3f** and Br–Pd–Br bond angles of 172.36(3)° and 174.26(3)° in **3e** and **3f**, respectively. The other bond angles in the coordination plane are almost perpendicular so as to adopt square planar geometry and in the range of 86.18(2)–93.82(2)° for all three complexes. Bond lengths around the metal center and N–$C_{carbene}$ bond lengths are similar to those reported for analogous: Pd–Br: 2.4159(17) Å, 2.4576(16) Å, Pd–$N_{pyridine}$: 2.095(9) Å, Pd–$C_{carbene}$: 1.959(10) Å, N–$C_{carbene}$ 1.335(13) Å, 1.355(14) Å.[14] For of each complex, dihedral angles between the mean planes of coordination plane, carbene and pyridine rings, which are denoted by *A*, *B* and *C* respectively, are given in the figure captions.

Suzuki–Miyaura cross coupling reactions

S–M cross-coupling reactions provide additional benefits in terms of designing safer processes. For instance, aromatic ketones can also be prepared effectively by cross-coupling reaction of arylboronic acid with acyl chloride. In the present study, the coupling reaction of phenylboronic acid and benzoyl chloride was selected as a model reaction to test the potential of NHC–Pd(II) complexes **2a–c** and **3b–f**, and the results are shown in Table 1. The reaction was performed in the presence of **2a–c** and **3b–f** as the catalyst and K_2CO_3 (1.5 mmol) in toluene (4 mL) at 60 °C under argon atmosphere for 4 h (Table 1, entries 1–10). Generally, PEPPSI type NHC–Pd(II) complexes **3b–f** displayed higher catalytic activity than $(NHC)_2PdBr_2$ complexes **2a–c**. The $(NHC)_2PdBr_2$ complexes **2b–c** were demonstrated moderate conversions (Table 1, entries 1–3). The catalytic conversions of NHC–Pd(II) complexes (**3b** and **3c**) were 88, and 96%, respectively (Table 1, entries 4 and 5). The chelate complex **3b′** had similar activity according to the non-chelated complex **3b** (Table 1, entry 6). When the effect of the position and number of the CN group in the catalyst structure on the catalytic activity was examined, significant differences were observed. Complex **3d** bearing 4-nitrile substituted benzyl group gave 69% yield (Table 1, entry 7). The increased number of nitrile groups in the catalyst did not cause a significant change in the catalytic activity (Table 1, entry 8). The complex **3e** showed similar activity to the complex **3c.** This showed that at least one CN group at position 2 in the ligand structure of the catalyst was sufficient for high activity. The complex **3f** without CN group gave the lowest catalytic activity (Table 1, entry 8). The complex **3c** exhibited better activity due to the high solubility in toluene when compared with the counterparts and reached 990 TON value. Unsatisfactorily, decreasing the catalyst loading to 0.05 mol% concluded 81% yield (Table 1, entry 11). In other reports, the authors mentioned that unidentified structures were detected in some catalytic reactions.[11] We also observed the undesired product and we found that this occurs when using aqueous solvents. In aqueous solvents, the benzoyl chloride converts the benzoic acid and thus directly affects the reaction efficiency. Eventually, this undesired product formation was minimized in the catalytic reaction with toluene (Table 1, entries 12–14). Reducing or increasing the temperature did not affect the conversion well (Table 1, entries 15 and 16). Replacing K_2CO_3 with KOH, NEt_3, NaOH, or $NaHCO_3$ resulted in a decrease in the conversion, but Cs_2CO_3 resulted in a good yield (Table 1, entries 17–21). However, K_2CO_3 was selected as a base for further studies due to its commercial and green advantages over Cs_2CO_3. Also, an inert atmosphere was required for the reaction (Table 1, entry 23). We also carried out control experiments to understand the progress of the reaction (Scheme 5). Control experiments without catalyst displayed no activity in the absence of the catalyst (Scheme 5, entry 1). In addition, the ligand has minimal effect to the activity without metal center (Scheme 5, entry 2). According to the *in situ* experiment, the yield of the reaction was reduced (Scheme 5, entry 3). In order to determine the activity of the acylative Suzuki–Miyaura coupling reaction, mercury poisoning and hot filtration experiments were performed for precatalyst **3c** using a one drop Hg (Scheme 5, entries 4 and 5). The mercury test showed a remarkable decrease in the conversion and only a 18% product formation was observed after 4 h. This result showed that the Pd nanoparticles were deactivated and the catalytic system took place in the heterogeneous nature. With the optimal reaction conditions determined, various arylboronic acids and benzoyl

Table 1 Optimization of reaction conditions for acylative Suzuki–Miyaura cross-coupling reaction of benzoyl chloride with phenylboronic acid[a]

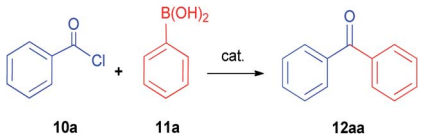

10a 11a 12aa

Entry	Cat.	Base	Solvent	Yield (%)
1	**2a**	K_2CO_3	Toluene	64
2	**2b**	K_2CO_3	Toluene	72
3	**2c**	K_2CO_3	Toluene	81
4	**3b**	K_2CO_3	Toluene	88
5	**3c**	K_2CO_3	Toluene	96
6	**3b′**	K_2CO_3	Toluene	86
7	**3d**	K_2CO_3	Toluene	69
8	**3e**	K_2CO_3	Toluene	85
9	**3f**	K_2CO_3	Toluene	58
10[b]	**3c**	K_2CO_3	Toluene	97
11[c]	**3c**	K_2CO_3	Toluene	81
12	**3c**	K_2CO_3	DCM	87
13	**3c**	K_2CO_3	Acetonitrile	44
14	**3c**	K_2CO_3	Acetone	53
15[d]	**3c**	K_2CO_3	Toluene	61
16[e]	**3c**	K_2CO_3	Toluene	25
17	**3c**	Cs_2CO_3	Toluene	99
18	**3c**	KOH	Toluene	89
19	**3c**	NEt_3	Toluene	30
20	**3c**	NaOH	Toluene	85
21	**3c**	$NaHCO_3$	Toluene	50
22[f]	**3c**	K_2CO_3	Toluene	89
23[g]	**3c**	K_2CO_3	Toluene	60

[a] Reaction conditions: benzoyl chloride (1.2 mmol), phenylboronic acid (1.0 mmol), base (1.5 mmol), solvent (4.0 mL), cat. 0.1 mol%, 60 °C, 4.0 h. [b] Cat. 0.5 mol%. [c] Cat. 0.05 mol%. [d] T = 110 °C. [e] Ambient temperature. [f] Toluene (2.0 mL). [g] Under air atmosphere. Isolated yields.

© 2021 The Author(s). Published by the Royal Society of Chemistry

Open Access Article. Published on 23 November 2021. Downloaded on 9/22/2024 3:55:22 AM.
This article is licensed under a Creative Commons Attribution-NonCommercial 3.0 Unported Licence.

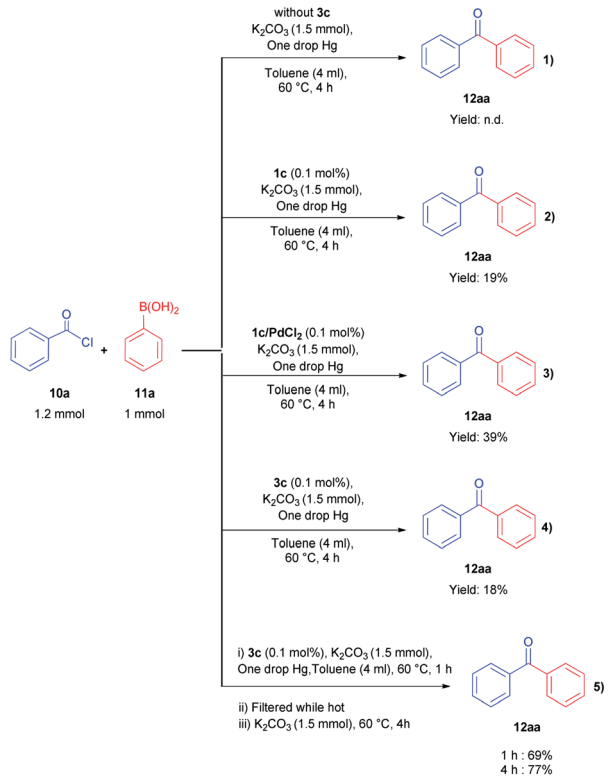

Scheme 5 Control experiments; (1) without catalyst, (2) only ligand, (3) *in situ* (4) mercury poisoning and (5) hot filtration for acylative Suzuki–Miyaura cross-coupling reaction. Isolated yields.

chlorides were investigated (Table 2). The reactions of benzoyl chloride with phenylboronic acid derivatives bearing 4-methyl, 2-methyl, and 2,4-dimethyl produced the corresponding products 4-methylbenzophenone, 2- methylbenzophenone, and 2,4-dimethylbenzophenone with yields of 88–94% (Table 2, entries 2–4). Accordingly, the reaction of phenylboronic acids bearing 4-Cl-2-CH_3, 2-F-4-OCF_3, 4-CN, and 4-CF_3 substituents with benzoyl chloride gave the desired products 4-chloro-2-methylbenzophenone, 2-fluoro-4-triflouromethoxybenzophenone, 4-cyanobenzophenone, and 4- trifluoromethylbenzophenone in 92–98% yields (Table 2, entries 5–8). We also explored the reactions between 4-nitrobenzoyl chloride and arylboronic acids. Arylboronic acids consisting of different substituents, 4-Cl-2-CH_3, 4-CF_3, and 4-Br, gave the corresponding products 4-chloro-2-methyl-4′-nitrobenzophenone, 4-trifluoromethyl-4′-nitrobenzophenone, and 4-bromo-4′-nitrobenzophenone with good yields of 93, 97 and 89%, respectively (Table 2, entries 9–11). Lastly, the reaction of 4-nitrobenzoyl chloride with phenylboronic acid resulted in 99% yield (Table 2, entry 12).

For a practical availability, gram-scale reaction was performed using benzoyl chloride (**10a**) with phenylboronic acid (**11a**), and benzophenone (**12aa**) was obtained in an 88% isolated yield (Scheme 6).

Nolan and Szostak developed [Pd(IPr)(μ-Cl)Cl]$_2$ catalyst for the acylative Suzuki–Miyaura cross-coupling reaction of aryl esters with phenylboronic acids.[35a] They revealed that the catalyst is the most reactive precatalysts among the other

Table 2 Acylative Suzuki–Miyaura cross-coupling reaction of acyl chlorides with arylboronic acids[a]

Entry	Arylboronic acids	Product	Yield (%)
1	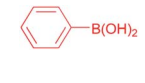	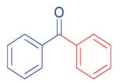	96
2	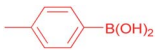	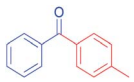	94
3	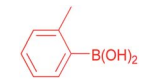	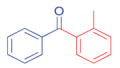	92
4	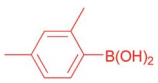	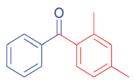	88
5	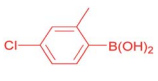	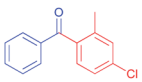	92
6	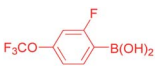	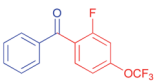	94
7	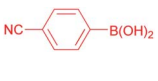	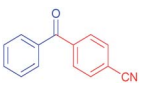	98
8	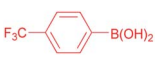	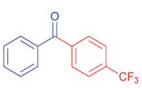	96
9	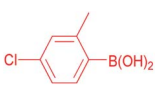	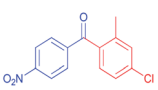	93
10	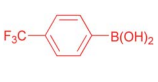	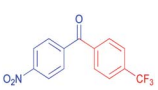	97
11	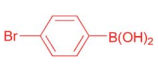	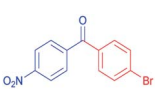	89
12	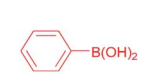	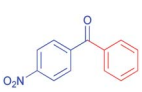	99

[a] Reaction conditions: benzoyl chloride (1.2 mmol), arylboronic acid (1.0 mmol), K_2CO_3 (1.5 mmol), 0.1 mol% cat., toluene (4.0 mL), 60 °C, 4.0 h. Benzoyl chloride was used for the entries 1–9, 4-nitro benzoyl chloride was used for the entries 10–12. Isolated yields.

catalyst in the literature for the reaction. Nolan and co-workers also reported Suzuki–Miyaura cross-coupling reactions of amides mediated by [Pd(NHC)(allyl)Cl] precatalysts to form biaryls.[35b]

Also, we explored the catalytic activity of NHC–Pd(II) complexes to test their potential in the Suzuki–Miyaura coupling reaction of bromobenzene with phenylboronic acids

Open Access Article. Published on 23 November 2021. Downloaded on 9/22/2024 3:55:22 AM.
This article is licensed under a Creative Commons Attribution-NonCommercial 3.0 Unported Licence.

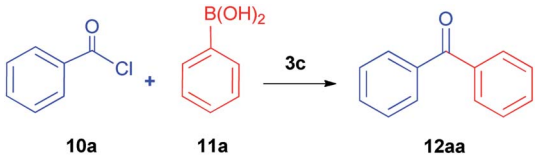

Scheme 6 Gram-scale synthesis of **12aa**[a]. [a] Reaction conditions: **10a** (1.68 g, 12.0 mmol), **11a** (1.22 g, 10.0 mmol), **3c** (0.1 mol%), K_2CO_3 (0.2 mg, 1.5 mmol), toluene (12.0 mL), 60 °C, 4 h, under argon atmosphere. Isolated yield.

(Table 3). The coupling reaction of bromobenzene and phenylboronic acid was selected as a benchmark reaction. The reaction was performed in the presence of **2a–c** and **3b–f** as the catalyst and KOH (0.5 mmol) in H_2O/2-propanol (2 mL) at 82 °C open to the air for 0.5 h (Table 3). All the synthesized catalysts (**2a–c**, **3b–f**) were tested in the reaction of bromobenzene with phenylboronic acid (Table 3, entries 1–9). Except for the complex **3f**, there was no significant difference between catalysts (Table 3, entry 9). The catalytic result of the complex **3f** demonstrated that the effect of the nitrile group was evident in the catalytic reaction. **3c** was decided as a catalyst for the Suzuki–Miyaura cross-coupling reaction of bromobenzene with phenylboronic acid. Reducing the catalyst loading also gave the satisfactory yield (Table 3, entry 10). The use of only water or 2-

Table 3 Suzuki–Miyaura cross-coupling reaction of bromobenzene with phenylboronic acid[a]

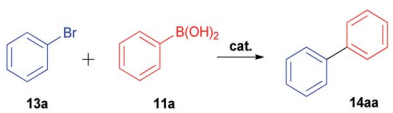

Entry	Cat.	Base	Solvent	Yield (%)
1	**2a**	KOH	H_2O/2-propanol	80
2	**2b**	KOH	H_2O/2-propanol	71
3	**2c**	KOH	H_2O/2-propanol	78
4	**3b**	KOH	H_2O/2-propanol	90
5	**3b′**	KOH	H_2O/2-propanol	88
6	**3c**	KOH	H_2O/2-propanol	94
7	**3d**	KOH	H_2O/2-propanol	79
8	**3e**	KOH	H_2O/2-propanol	89
9	**3f**	KOH	H_2O/2-propanol	53
10[b]	**3c**	KOH	H_2O/2-propanol	85
11	**3c**	KOH	2-Propanol	68
12	**3c**	KOH	H_2O	72
13	—	KOH	H_2O/2-propanol	2
14	**3c**	$NaHCO_3$	H_2O/2-propanol	45
15	**3c**	Cs_2CO_3	H_2O/2-propanol	81
16	**3c**	NaOH	H_2O/2-propanol	64
17	**3c**	KO^{t}Bu	H_2O/2-propanol	62
18	**3c**	K_2CO_3	H_2O/2-propanol	73
19[c]	**3c**	KOH	H_2O/2-propanol	68
20[d]	**3c**	KOH	H_2O/2-propanol	9

[a] Reaction conditions: bromobenzene (1.0 mmol), phenylboronic acid (1.0 mmol), KOH (0.5 mmol), cat. (0.2 mol%), 82 °C, 2 mL solvent or 0.5 mL 2-propanol + 1.5 mL H_2O, 0.5 h, under air. [b] Cat. 0.1 mol%. [c] 60 °C. [d] 24 °C. Isolated yields.

Table 4 Suzuki–Miyaura cross-coupling reaction of aryl bromides with arylboronic acids[a]

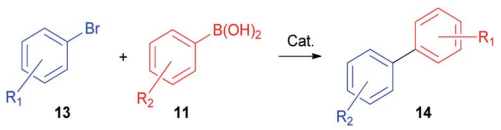

Entry	Arylboronic acid (**11**)	Product (**14**)	Yield (%)
1	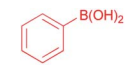		85
2		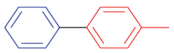	71
3	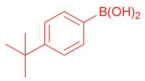	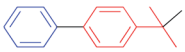	66
4	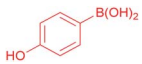	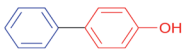	71
5		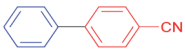	74
6	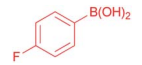	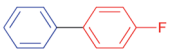	91
7	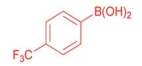	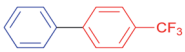	92
8	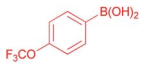	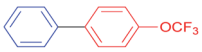	81
9	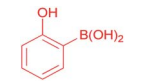	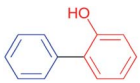	55
10	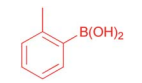	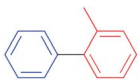	59
11	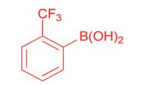		52
12	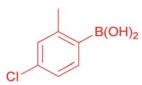	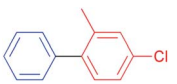	85
13	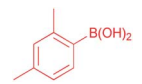	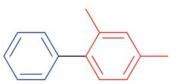	53
14	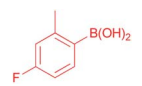	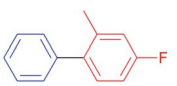	77
15	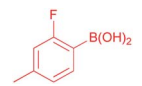	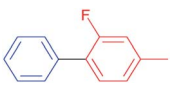	45
16	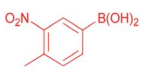	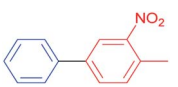	65
17	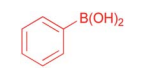	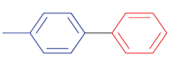	77

© 2021 The Author(s). Published by the Royal Society of Chemistry

Open Access Article. Published on 23 November 2021. Downloaded on 9/22/2024 3:55:22 AM. This article is licensed under a Creative Commons Attribution-NonCommercial 3.0 Unported Licence.

Table 4 (*Contd.*)

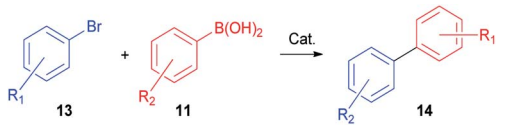

Entry	Arylboronic acid (**11**)	Product (**14**)	Yield (%)
18	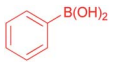	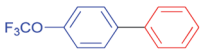	70

[a] Reaction conditions: aryl bromide (1.0 mmol), arylboronic acid (1.0 mmol), KOH (0.5 mmol), **3c** (0.2 mol%), 0.5 mL 2-propanol + 1.5 mL H_2O, 82 °C, 0.5 h, under air. Isolated yields.

propanol as solvent negatively affected the conversion (Table 3, entries 11 and 12). No product formation was observed in the absence of the catalyst (Table 3, entry 13). The formation of biphenyl was reduced in the presence of different bases such as $NaHCO_3$, NaOH, KO^{t}Bu, and K_2CO_3, while the emulative yield was observed with Cs_2CO_3 (Table 3, entries 14–18). Decreasing the temperature resulted in lower conversions (Table 3, entries 19 and 20). Assessment of the substrate scope of the reaction of various phenylboronic acids with bromobenzene, 4-bromotoluene, and 4-bromoanisole was performed under the optimized reaction conditions (Table 4). Numerous arylboronic acids bearing electron-withdrawing or electron-donating substituents at the *para*-position such as 4-CH_3, 4-*tert*-butyl, 4-OH, 4-CN, 4-F, 4-CF_3, and 4-OCF_3 were converted into the corresponding biphenyls namely 4-methyl-biphenyl, 4-(*tert*-butyl)-biphenyl, 4-hydroxy-biphenyl, 4-cyano-biphenyl, 4-fluorobiphenyl, 4-(trifluoromethyl)-biphenyl, and 4-(trifluoromethoxy)-biphenyl in high yields (Table 4, entries 2–8). But, *ortho*-substituted phenylboronic acids like 2-OH, 2-Me and 2-CF_3 gave the desired products 2-methyl-biphenyl, 4-hydroxy-biphenyl, and 2-(trifluoromethyl)-biphenyl with a average isolated yields (Table 4, entries 9–11). The double-substituted phenylboronic acids such as 4-Cl-2-Me, 2,4-dimethyl, 4-F-3-Me, 2-F-4-Me, and 4-Me-3-NO_2 resulted in good yields in the coupling reactions with the products of 4-chloro-2-methyl-biphenyl, 2,4-dimethyl-biphenyl, 4-fluoro-3-methyl-biphenyl, 2-fluoro-4-methyl-biphenyl, and 4-methyl-3-nitro-biphenyl (Table 4, entries 12–16). Furthermore, different aryl bromides were also examined. Aryl bromides consisting of electron-withdrawing substituents, 4-CH_3 and 4- OCH_3, gave the corresponding products 4-methyl-biphenyl and 4-methoxy-biphenyl with good yields of 77 and 70%, respectively (Table 4, entries 17, 18). For a practical availability, gram-scale reaction was performed using bromobenzene (**13a**) with phenylboronic acid (**11a**), and biphenyl was obtained in an 86% isolated yield (Scheme 7).

Kajetanowicz *et al.* developed catalysts possessing quinone moieties in the pyridine ligand for the Suzuki–Miyaura cross-coupling reaction of phenylboronic acid with 3,5-dimethoxy-bromobenzene.[36] They drew attention to the similarity of the steric and electronic properties of the Organ's Pd–PEPPSI catalysts.

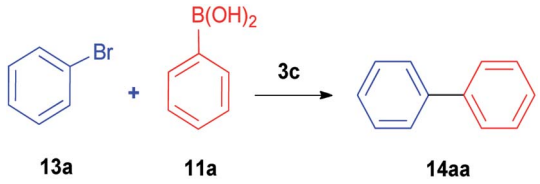

Scheme 7 Gram-scale synthesis of **14aa**[a]. [a] Reaction conditions: **13a** (1.57 g, 10.0 mmol), **11a** (1.22 g, 10.0 mmol), **3c** (0.1 mol%), KOH (28 mg, 0.5 mmol), 0.5 mL 2-propanol + 1.5 mL H_2O, 82 °C, under air atmosphere. Isolated yield.

Scanning Electron Microscopy (SEM), energy dispersive X-ray spectroscopy (EDS) and metal mapping analyses were performed to get further insights into the mechanism of the Suzuki–Miyaura cross coupling reactions (Fig. 4 and 5). Au was coated on the surface of the Pd nanoparticles to prevent the specimen from charging during analysis. The black precipitates were collected by filtration at the end of the catalytic reactions and washed with plenty of water. The Pd nanoparticles appeared as cluster with the sizes ranging from 45 to 60 nm for both reaction. EDS and metal mapping images of the black precipitates clearly proven the presence of Pd atom (Fig. 5). Also, the images displayed N and C atoms which are most probably attributed to the NHC ligand. The other atoms like K and O are impurities remaining from the salts (KOH or K_2CO_3).

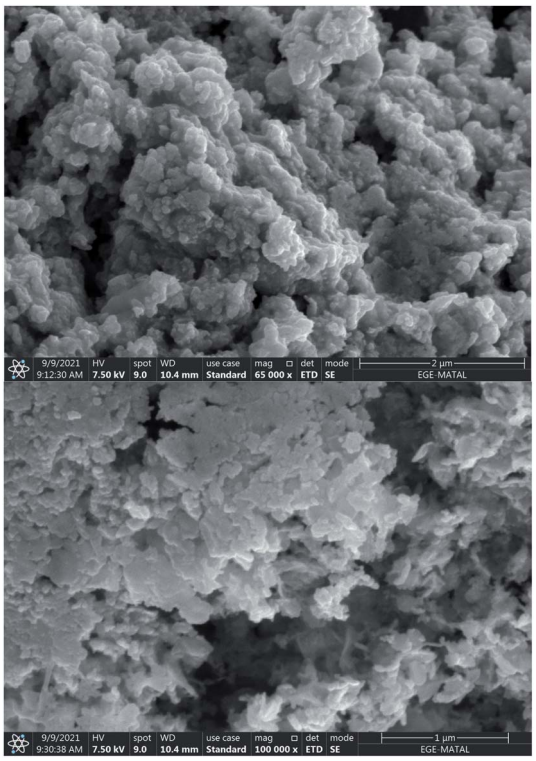

Fig. 4 SEM images of Pd nanoparticles for acylative Suzuki–Miyaura coupling reaction of benzoyl chloride with phenylboronic acid (top) and Suzuki–Miyaura cross-coupling reaction of phenylboronic acid with bromobenzene (bottom).

© 2021 The Author(s). Published by the Royal Society of Chemistry

Open Access Article. Published on 23 November 2021. Downloaded on 9/22/2024 3:55:22 AM.
This article is licensed under a Creative Commons Attribution-NonCommercial 3.0 Unported Licence.

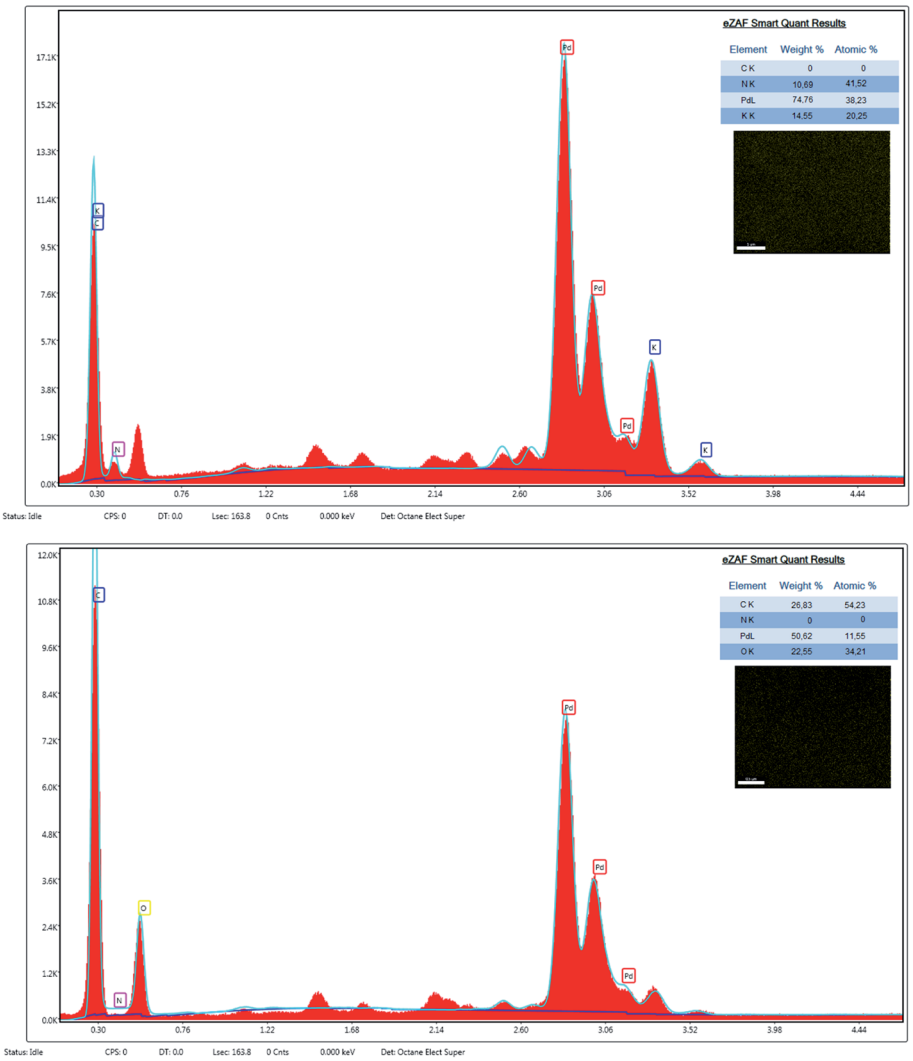

Fig. 5 EDS and metal mapping images of Pd nanoparticles for acylative Suzuki–Miyaura coupling reaction of benzoyl chloride with phenylboronic acid (top) and Suzuki–Miyaura cross-coupling reaction of phenylboronic acid with bromobenzene (bottom).

The possible mechanisms of the Suzuki–Miyaura coupling reactions are summarized in Scheme 8. Both reaction mechanisms conducted through the classical Suzuki–Miyaura C–C coupling reaction mechanism, which includes the pre-activation, oxidative addition, transmetalation, and reductive elimination, respectively. Pre-activation occurs with the effect of base, solvent or temperature, and the pre-activation of the catalyst is the state with the least energy profile.[32] The steric hindrance from NHC ligands plays an important role in the activation process of the catalyst.[35b] The leaving group (halogen) and ligands are more crucial than metal center in the pre-activation. Since bromine is an easily leaving group, the pre-activation process is faster.[35c] However, there may be slight differences in the mechanism due to optimization conditions.[16] In the cross-coupling reaction, the possibility of attachment of the hydroxyl group to the palladium center is high due to the use of hydroxyl-containing base (KOH) and water as solvent. In our last study, we supported this attachment with the computational study.[15] But, in the acylative cross-coupling reaction, as we have stated before, there must not be any water in the reaction conditions to avoid by-product formation, which reduces the possibility of Pd–OH bond formation. Of course, the formation of Pd–CO_3 interaction as an intermediate is expected due to K_2CO_3.[33] The main purpose of the base in Suzuki–Miyaura cross-coupling reactions is to break the Pd–halide bond by increasing the reactivity of boronic acid in the transmetalation step.[34]

We supported removal of the pyridine group during the catalytic cycle by thermogravimetric analysis (TGA) (ESI†). The TGA spectrum of the complex **3c** showed a band around 210 °C which is attributed to the pyridine group.[27] This band did not appear in the TGA spectrum of the nanoparticle of **3c**, indicating the absence of pyridine in the nanostructure (Fig. S60 and S61†). In addition, Dyson *et al.* reported that the nitrile group has two important roles, which are forming a protective group around the nanoparticle and helping to stabilize the active Pd(II) catalyst.[28] Both TGA spectrum displayed a band around 305 °C which are attributed to the NHC ligand. This

© 2021 The Author(s). Published by the Royal Society of Chemistry

Open Access Article. Published on 23 November 2021. Downloaded on 9/22/2024 3:55:22 AM.
This article is licensed under a Creative Commons Attribution-NonCommercial 3.0 Unported Licence.

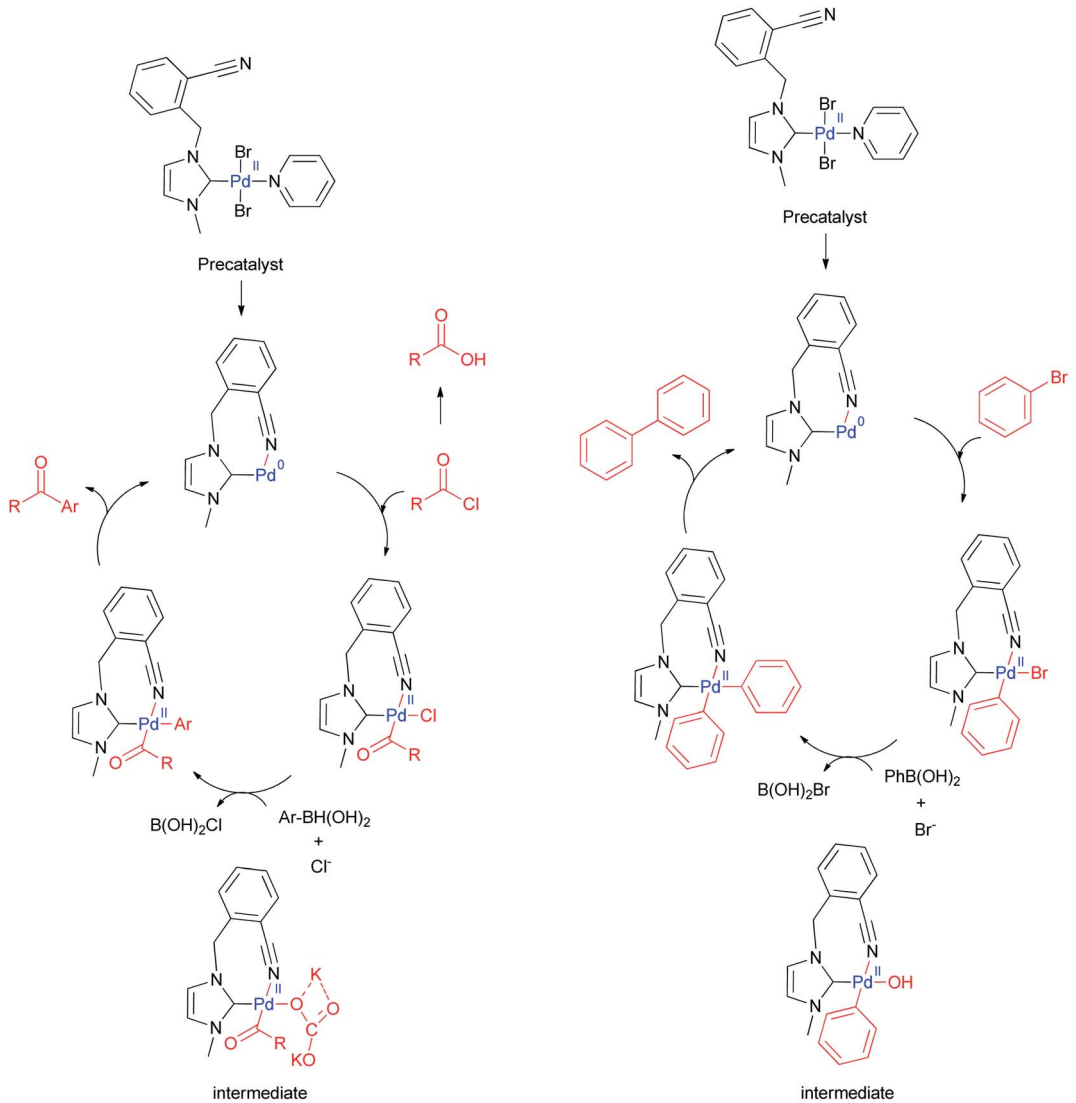

Scheme 8 Proposed mechanisms of Suzuki–Miyaura acylative-coupling reaction and cross-coupling reaction with **3c**.

demonstrated that the NHC ligand remains stable in the Pd nanoparticles. Also, the FT-IR spectrum of the Pd nanoparticles depicted the presence of the nitrile group (Fig. S62†).

NHC ligands with electron-rich and steric groups can make subtle changes to the electronic and steric effect of the palladium center.[29] The advantages of the electronic and steric effects arising from NHC ligands to the complex are as follows: remarkable activity in the catalytic process, formation of stable complexes against air and moisture, uniquely strong σ-donor feature, wide range scope.[30] Pd–PEPPSI–IPr complexes have also been good alternatives to classical Pd–PEPPSI–NHC complexes in C–C and C–N bond formation reactions.[31] The steric affects of IPr ligands would improve the efficiency of reductive elimination step. NHC ligands are an influencing factor in determining which step in the cycle is rate limiting.[31c] Bulky and flexible NHC ligands such as IPr can overcome several limitations of cross-coupling reactions.[31d] The most important classes of the PEPPSI type Pd catalysts containing NHC ligand was developed by Organ.[37] Our Pd-PEPPSI catalysts with nitrile moiety offer comparable results to conventional catalysts in the literature for Suzuki–Miyaura cross-coupling reactions.

Conclusions

In conclusion, a series of CN-containing azolium salts and their palladium complexes were synthesized as the model compounds to systematically study the effect of CN substituents on the both Suzuki–Miyaura cross-coupling reactions. $(NHC)_2$-$PdBr_2$ (**2a–c**) and PEPPSI type (NHC)Pd(II) (**3b–f**) complexes were used to give C(acyl)–C(sp^2) and C(sp^2)–C(sp^2) Suzuki–Miyaura cross-coupling reactions to yield the corresponding carbonyl compounds and biphenyls, respectively. By introducing the CN substituents onto the phenylene ring of NHC in the Pd complexes, both activity and stability of the resulting nanocatalysts are greatly enhanced. The complex (**3c**) which has imidazole as the NHC skeleton, and 2-CN benzyl and methyl as the side groups generated higher activity in both catalytic reactions. The SEM analysis, EDS and metal mapping analysis,

© 2021 The Author(s). Published by the Royal Society of Chemistry

Open Access Article. Published on 23 November 2021. Downloaded on 9/22/2024 3:55:22 AM.
This article is licensed under a Creative Commons Attribution-NonCommercial 3.0 Unported Licence.

mercury drop tests and poison experiments of the catalytic solution showed that (NHC)Pd was involved in catalysis. The synthesis of transition metal NHC complexes containing CN group and their different catalytic applications are currently under investigation.

Experimental

X-ray crystallography

X-ray single-crystal diffraction data for complexes **3e**, **3f** and **3c** were collected at 294(2) K on a Rigaku-Oxford Xcalibur diffractometer with an Eos-CCD detector using graphite-monochromated MoKα radiation (λ = 0.71073 Å). Details of the data collection conditions and refinement processes are summarized in Table S1, as ESI†. For each compound, data reduction and analytical absorption corrections were performed using CrysAlisPro 1.171.40.67a software.[17] The structure was solved with the ShelXT[18] solution program using dual methods and by using Olex2 (ref. 19) as the graphical interface. The model was refined with ShelXL2018/3 (ref. 20) using full matrix least squares minimization on F2. All non-hydrogen atoms were refined as isotropically. Hydrogen atom positions were calculated geometrically and refined using the riding model, fixing the aromatic C–H distances at 0.93 Å, methylene C–H distances at 0.97 Å, methyl C–H distances at 0.96 Å. U_{iso}(H) values were set to 1.2 U_{eq} (1.5 U_{eq} for the methyl group) of the parent atom. Atom Br4 in complex **3f** is disordered over two sets of sites, with a refined occupancy ratio of 0.661(13) : 0.339(13). CCDC 2071690, 2071692, 2071693 contain the supplementary crystallographic data for **3e**, **3f** and **3c**, respectively.

Materials

Unless otherwise noted, all operations were performed without taking precautions to exclude air and moisture. The glass equipment was heated under vacuum in order to remove oxygen and moisture and then they were filled with argon. Starting compounds and reagents were obtained from Merck, Fluka, Alfa Aesar and Acros Organics; pyridine, $PdCl_2$ were obtained from Alfa Aesar and dichloromethane, acetonitrile, ethanol, diethyl ether, toluene, pyridine were obtained from Merck and Ridel de Haen. Catalytic reactions for Suzuki–Miyaura cross-coupling reactions were carried out under argon gas on Carousel 12 Plus Reaction Station system. ^{1}H and ^{13}C NMR spectra were recorded on a Varian AS 400 Mercury instrument. FTIR spectra were recorded on a PerkinElmer Spectrum 100 series. Scanning Electron Microscopy (SEM), energy dispersive X-ray spectroscopy (EDS) and metal mapping analyses were collected on a Thermo Scientific Apreo S.

Synthesis of compound 1a. Benzothiazole (1.00 g, 7.39 mmol) was dissolved in 5 mL of toluene and 2-bromobenzonitrile (1.45 g, 7.39 mmol) was added to boil under reflux for 24 h. The precipitate is then filtered off and washed with diethyl ether. Dried under vacuum to yield. Yield = 81%, 1.98 g. ^{1}H NMR (400 MHz, DMSO-d_6): δ 10.8 (s, 1H, S–CH–N), 8.59 (m, 1H, J = 2 Hz, Ar-H), 8.17 (m, 1H, Ar-H), 7.99 (d, J = 7.6 Hz, 1H, Ar-H), 7.86 (m, 2H, Ar-H), 7.69 (t, J = 8 Hz, 1H, Ar-H), 7.67 (t, J = 7.6 Hz, 1H, Ar-H), 7.31 (d, J = 8 Hz, 1H, Ar-H), 6.40 (s, 2H, N–CH_2). ^{13}C NMR (100 MHz, DMSO-d_6): δ 167.6, 140.7, 136.5, 134.5, 134.4, 132.2, 130.1, 128.9, 126.1, 117.5, 111.1, 54.1. IR, ν_{max} (cm^{-1}) (CH_2Cl_2): 3367, 3091, 3061, 3021, 2978, 2939, 2897, 2221, 1987, 1682, 1594, 1577, 1493, 1462, 1448, 1426, 1293, 1209, 1175, 1094, 1080, 1032, 900, 834, 792, 774, 760, 751, 730, 643, 597, 581, 512, 452, 425, 404.

Synthesis of compound 1b. Prepared according to procedure **1a** using 1-methylbenzimidazole (1.00 g, 7.56 mmol) and 2-bromobenzonitrile (1.48 g, 7.56 mmol). Yield = 85%, 2.12 g. ^{1}H NMR (400 MHz, $CDCl_3$): δ 9.84 (s, 1H, NCHN), 8.08 (d, J = 8 Hz, 1H, Ar-H), 7.98 (d, J = 7.6 Hz, 1H, Ar-H), 7.88 (d, J = 8 Hz, 1H, Ar-H), 7.69 (m, 3H, Ar-H), 7.59 (t, J = 7.6 Hz, 1H, Ar-H), 7.45 (d, J = 7.6 Hz, 1H, Ar-H), 6.03 (s, 2H, N–CH_2), 4.13 (s, 3H, N–CH_3). ^{13}C NMR (100 MHz, $CDCl_3$): δ 144.0, 137.5, 134.4, 134.2, 132.4, 131.4, 129.9, 129.4, 127.4, 127.2, 117.4, 114.4, 113.9, 111.3, 48.6, 33.9. IR, ν_{max} (cm^{-1}) (CH_2Cl_2): 3810, 3430, 3137, 3096, 3006, 2979, 2925, 2904, 2843, 2772, 2652, 2584, 2431, 2223, 1967, 1920, 1873, 1807, 1784, 1729, 1696, 1610, 1599, 1570, 1485, 1444, 1366, 1345, 1292, 1277, 1216, 1209, 1165, 1128, 1088, 1047, 1028, 1008, 989, 964, 906, 847, 787, 774, 759, 746, 686, 609, 582, 559, 448, 420.

Synthesis of compound 1c. Prepared according to procedure **1a** using 1-methylimidazole (1.00 g, 12.0 mmol) and 2-bromobenzonitrile (2.38 g, 12.0 mmol). Yield = 89%, 3.02 g. ^{1}H NMR (400 MHz, $CDCl_3$): δ 10.2 (s, 1H, NCHN), 7.92 (d, J = 7.6 Hz, 1H, Ar-H), 7.71 (s, 1H, Ar-H), 7.59 (m, 2H, Ar-H), 7.51 (s, 1H, NCHCHN), 7.43 (t, J = 7.6 Hz, 1H, NCHCHN), 5.80 (s, 2H, N–CH_2), 4.00 (s, 3H, N–CH_3). ^{13}C NMR (100 MHz, $CDCl_3$): δ 182.2, 137.4, 136.5, 134.3, 133.4, 131.1, 130.1, 124.3, 122.3, 117, 0, 112.0, 50.8, 37.0. IR, ν_{max} (cm^{-1}) (CH_2Cl_2): 3487, 3136, 3084, 3030, 2950, 2919, 2885, 2843, 2407, 2227, 2000, 1740, 1657, 1599, 1572, 1561, 1490, 1451, 1366, 1339, 1298, 1285, 1212, 1169, 1162, 1095, 1082, 962, 887, 866, 824, 775, 652, 622, 557, 477, 447, 404.

Synthesis of compound 1d. Prepared according to procedure **1a** using 1-methylimidazole (1.00 g, 12.0 mmol) and 4-bromobenzonitrile (2.38 g, 12.0 mmol). Yield = 59%, 2.00 g. ^{1}H NMR (400 MHz, DMSO-d_6): δ 9.33 (s, 1H, NCHN), 7.89 (d, J = 7.6 Hz, 2H, Ar-H), 7.83 (s, 1H, NCHCHN), 7.76 (s, 1H, NCHCHN), 7.60 (d, J = 8 Hz, 2H, Ar-H), 5.57 (s, 2H, N–CH_2), 3.86 (s, 3H, N–CH_3). ^{13}C NMR (100 MHz, DMSO-d_6): δ 166.6, 140.4, 138.8, 133.4, 132.3, 130.2, 129.5, 128.9, 126.0, 118.8, 117.7, 112.1, 54.9. IR, ν_{max} (cm^{-1}) (CH_2Cl_2): 3418, 3060, 2965, 2910, 2221, 1599, 1510, 1483, 1454, 1379, 1357, 1314, 1284, 1270, 1207, 1141, 1116, 1053, 1029, 982, 913, 793, 762, 713, 674, 604, 552, 450, 432.

Synthesis of compound 1e. Imidazole (1.00 g, 14.68 mmol) was dissolved in 5 mL ethanol and mixed with NaOH for 30 min. 2-Bromobenzonitrile (5.76 g, 29.36 mmol) was then added to the mixture and boiled under reflux for 24 hours. The precipitate is then filtered and washed with diethyl ether. It was dried under vacuum. Yield = 72%, 4.02 g. ^{1}H NMR (400 MHz, DMSO-d_6): δ 9.41 (s, 1H, NCHN), 7.95 (d, J = 10.8 Hz, 2H, Ar-H), 7.87 (d, J = 1.6 Hz, 2H, Ar-H), 7.78 (t, J = 5.2 Hz, 2H, Ar-H), 7.61 (t, J = 7.6 Hz, 2H, Ar-H), 7.48 (d, J = 7.6 Hz, 2H, NCHCHN), 5.74 (s, 4H, N–CH_2). ^{13}C NMR (100 MHz, DMSO-d_6): δ 138.3, 137.9, 134.5, 134.1, 130.1, 129.7, 123.9, 117.3, 111.3, 50.9. IR, ν_{max} (cm^{-1})

© 2021 The Author(s). Published by the Royal Society of Chemistry

Open Access Article. Published on 23 November 2021. Downloaded on 9/22/2024 3:55:22 AM. This article is licensed under a Creative Commons Attribution-NonCommercial 3.0 Unported Licence.

(CH_2Cl_2): 3792, 3414, 3168, 3129, 3044, 3022, 2861, 2222, 1756, 1643, 1617, 1599, 1566, 1487, 1438, 1348, 1303, 1288, 1213, 1182, 1170, 1095, 1045, 1024, 978, 953, 883, 858, 819, 765, 700, 638, 557, 467, 465.

Synthesis of compound 1f. Prepared according to procedure **1a** using 1-methylimidazole (1.00 g, 12.0 mmol) and benzoyl bromide (2.25 g, 12.0 mmol). Yield = 73%, 3.23 g. ^{1}H NMR (400 MHz, DMSO-d_6): δ 9.41 (s, 1H, NCHN), 7.85 (d, J = 1.6 Hz, 1H, NCHCHN), 7.75 (d, J = 1.2 Hz, 1H, NCHCHN), 7.45 (d, J = 6.4 Hz, 2H, Ar-H), 7.40 (d, J = 7.2 Hz, 2H, Ar-H), 7.35 (m, 1H, Ar-H), 5.47 (s, 2H, N–CH_2), 3.86 (s, 3H, N–CH_3). ^{13}C NMR (100 MHz, DMSO-d_6): δ 137.0, 135.4, 129.4, 129.1, 128.8, 124.4, 122.7, 52.1, 36.4. IR, ν_{max} (cm^{-1}) (CH_2Cl_2): 3418, 3148, 3090, 2063, 1626, 1573, 1562, 1497, 1456, 1427, 1388, 1362, 1335, 1208, 1161, 1108, 1083, 1029, 1002, 853, 822, 722, 699, 662, 622, 466.

Synthesis of complex 2a. In balloon, **1a** (0.50 g, 1.51 mmol) and Ag_2O (0.18 g, 0.76 mmol) under argon gas was suspend in acetonitrile (5 mL) and stirred at room temperature for 12 h protected from light. Then, $[PdCl_2(CH_3CN)]_2$ (0.19 g, 0.76 mmol) was added over and the reflux 24 h. The solid residue remained was washed with diethyl ether. Then dried under vacuum. Yield = 46%, 0.53 g. ^{1}H NMR (400 MHz, $CDCl_3$): δ 7.71 (d, J = 7.2 Hz, 2H, Ar-H), 7.51 (t, J = 8 Hz, 2H, Ar-H), 7.46 (d, J = 8 Hz, 2H, Ar-H), 7.39 (t, J = 7.6 Hz, 2H, Ar-H), 7.24 (m, 4H, Ar-H), 7.17 (t, J = 7.6 Hz, 2H, Ar-H), 6.93 (d, J = 7.6 Hz, 2H, Ar-H), 5.38 (s, 4H, N–CH_2). ^{13}C NMR (100 MHz, $CDCl_3$): δ 170.3, 138.8, 136.3, 133.6, 133.1, 128.4, 127.3, 126.7, 123.8, 122.8, 122.5, 117.1, 111.2, 110.9, 43.9. IR, ν_{max} (cm^{-1}) (CH_2Cl_2): 3791, 3663, 3347, 3068, 2930, 2224, 2190, 1954, 1905, 1767, 1692, 1588, 1561, 1483, 1471, 1447, 1424, 1358, 1352, 1325, 1305, 1285, 1260, 1205, 1197, 1183, 1092, 1044, 1019, 979, 957, 931, 884, 851, 809, 766, 751, 717, 693, 660, 622, 582, 557, 545, 502, 482, 464, 443, 429.

Synthesis of complex 2b. Prepared according to procedure **2a** using **1b** (0.50 g, 1.52 mmol), Ag_2O (0.18 g, 0.76 mmol) and $[PdCl_2(CH_3CN)]_2$ (0.19 g, 0.76 mmol). Yield = 35%, 0.40 g. ^{1}H NMR (400 MHz, DMSO-d_6): δ 8.01–7.96 (dd, J = 7.6 Hz, 2H, Ar-H), 7.84–7.76 (dd, J = 8 Hz, 2H, Ar-H), 7.44 (m, 10H, Ar-H), 7.17 (m, 2H, Ar-H), 6.36–6.32, 6.12–6.08 (dd, J = 16.8 MHz, 2H, N–CH_2), 6.42 (s, 2H, N–CH_2), 4.31 (d, J = 8.8 Hz, 6H, N–CH_3). ^{13}C NMR (100 Hz, DMSO-d_6): δ 139.4, 139.2, 134.6, 134.5, 133.9, 133.9, 133.8, 133.7, 129.4, 129.2, 128.8, 128.6, 128.3, 124.8, 124.7, 124.3, 124.2, 118.5, 117.8, 117.7, 112.3, 111.9, 111.6, 111.4, 111.2, 111.1, 49.8, 49.6, 35.6, 35.4. IR, ν_{max} (cm^{-1}) (CH_2Cl_2): 3436, 2920, 2294, 2224, 1737, 1599, 1484, 1452, 1413, 1355, 1211, 1107, 1030, 986, 824, 798, 762, 559, 447.

Synthesis of complex 2c. Prepared according to procedure **2a** using **1c** (0.50 g, 1.80 mmol), Ag_2O (0.21 g, 0.90 mmol) and $[PdCl_2(CH_3CN)]_2$ (0.23 g, 0.90 mmol). Yield = 18%, 0.25 g. ^{1}H NMR (400 MHz, DMSO-d_6): δ 7.95–7.91 (dd, J = 7.6 Hz, 2H, Ar-H), 7.67 (t, J = 7.6 Hz, 2H, Ar-H), 7.51 (m, 6H, Ar-H), 7.35–7.29 (dd, J = 8 Hz, 2H, Ar-H), 5.88–5.84, 5.77–5.73 (dd, J = 16.0 Hz, 2H, N–CH_2), 5.83 (s, 2H, N–CH_2), 3.99 (d, J = 9.6 Hz, 6H, N–CH_3). ^{13}C NMR (100 MHz, DMSO-d_6): δ 179.3, 139.9, 134.0, 133.7, 129.5, 129.0, 124.9, 123.9, 117.7, 111.3, 51.7, 37.9. IR, ν_{max} (cm^{-1}) (CH_2Cl_2): 3317, 3105, 2926, 2222, 1676, 1602, 1571, 1470, 1244, 1218, 1199, 1135, 1079, 943, 762, 732, 689, 657, 458.

Synthesis of complex 3b. In balloon, **1b** (0.50 g, 1.52 mmol) under argon gas was pyridine (3 mL) dissolved. Then, $PdCl_2$ (0.27 g, 1.52 mmol) and K_2CO_3 (1.05 g, 7.62 mmol) was added and refluxed overnight. The solid residue remained was washed with diethyl ether. Then dried under vacuum. Yield = 56%, 0.51 g. ^{1}H NMR (400 MHz, $CDCl_3$): δ 9.04 (d, J = 1.6 Hz, 2H, Py-H), 7.78 (m, 2H, Py-H), 7.71 (d, J = 8.8 Hz, 1H, Py-H), 7.50 (t, J = 8 Hz, 1H, Ar-H), 7.42 (m, 2H, Ar-H), 7.37 (m, 2H, Ar-H), 7.31 (t, J = 8 Hz, 1H, Ar-H), 7.20 (m, 1H, Ar-H), 7.11 (m, 1H, Ar-H), 6.36 (s, 2H, N–CH_2), 4.40 (s, 3H, N–CH_3). ^{13}C NMR (100 MHz, CDC_{l3}): δ 164.8, 152.6, 151.9, 138.5, 138.1, 135.4, 133.9, 133.4, 132.9, 129.5, 128.6, 124.6, 123.6, 117.3, 111.4, 110.7, 110.3, 50.4, 35.5. IR, ν_{max} (cm^{-1}) (CH_2Cl_2): 3381, 3059, 2926, 2223, 1692, 1603, 1539, 1499, 1446, 1403, 1348, 1295, 1253, 1190, 1153, 1126, 1098, 1070, 1011, 919, 803, 760, 691, 668, 558, 439.

Complex 3b′. Yield = 32%, 0.41 g. ^{1}H NMR (400 MHz, $CDCl_3$): δ 7.69 (d, J = 7.2 Hz, 1H, Ar-H), 7.50 (t, J = 7.2 Hz, 1H, Ar-H), 7.37 (t, J = 7.6 Hz, 2H, Ar-H), 7.12 (t, J = 7.6 Hz, 1H, Ar-H), 7.03 (m, 2H, Ar-H), 7.93 (d, J = 7.6 Hz, 1H, Ar-H), 5.31 (s, 2H, N–CH_2), 3.49 (s, 3H, N–CH_3). ^{13}C NMR (100 MHz, $CDCl_3$): δ 154.5, 153.3, 140.1, 133.4, 132.9, 130.1, 128.6, 128.3, 128.2, 124.9, 121.8, 121.6, 117.3, 111.3, 108.1, 107.7, 42.7, 29.7, 27.4. IR, ν_{max} (cm^{-1}) (CH_2Cl_2): 3527, 3444, 3379, 3059, 2926, 2222, 1691, 1601, 1541, 1499, 1401, 1341, 1295, 1254, 1210, 1191, 1154, 1100, 1068, 1013, 920, 796, 761, 744, 692, 658, 442.

Synthesis of complex 3c. Prepared according to procedure **3b** using **1c** (0.50 g, 1.79 mmol), $PdCl_2$ (0.32 g, 1.79 mmol) and K_2CO_3 (1.24 g, 8.99 mmol). Yield = 65%, 0.63 g. ^{1}H NMR (400 MHz, $CDCl_3$): δ 9.00–8.99 (dd, J = 1.6 Hz, 2H, Py-H), 7.94 (d, J = 7.6 Hz, 1H, Ar-H), 7.75 (m, 2H, Py-H), 7.60 (dt, J = 7.6 Hz, 1H, Py-H), 7.45 (dt, J = 7.6 Hz, 1H, Ar-H), 7.33 (m, 2H, Ar-H), 6.97–6.94 (dd, J = 2 Hz, 2H, N–CHCH–N), 5.97 (s, 2H, N–CH_2), 4.14 (s, 3H, N–CH_3). ^{13}C NMR (100 MHz, $CDCl_3$): δ 154.3, 152.5, 150.1, 139.0, 138.4, 137.9, 133.4, 132.9, 130.9, 128.9, 124.9, 124.7, 123.9, 122.2, 112.2, 52.4, 38.7. IR, ν_{max} (cm^{-1}) (CH_2Cl_2): 3437, 3161, 3127, 3104, 2944, 2219, 1706, 1640, 1603, 1567, 1484, 1468, 1445, 1415, 1366, 1327, 1293, 1280, 1247, 1211, 1193, 1148, 1068, 1046, 1018, 943, 795, 767, 731, 684, 643, 552, 447, 431.

Synthesis of complex 3d. Prepared according to procedure **3b** using **1d** (0.50 g, 1.79 mmol), $PdCl_2$ (0.32 g, 1.79 mmol) and K_2CO_3 (1.24 g, 8.99 mmol). Yield = 38%, 0.36 g. ^{1}H NMR (400 MHz, DMSO-d_6): δ 8.79 (d, J = 5.6 Hz, 2H, Py-H), 7.95 (d, J = 5.6 Hz, 1H, Py-H), 7.85 (d, J = 8 Hz, 2H, Ar-H), 7.66 (d, J = 7.6 Hz, 2H, Py-H), 7.51 (s, 2H, N–CHCH–N), 7.44 (s, 1H, Ar-H), 7.31 (d, J = 3.2 Hz, 1H, Ar-H), 5.80 (d, J = 9.6 Hz, 2H, N–CH_2), 4.01 (t, J = 8 Hz, 3H, N–CH_3). ^{13}C NMR (100 MHz, DMSO-d_6): δ 152.4, 151.9, 132.8, 129.8, 129.7, 129.6, 125.4, 122.9, 119.2, 111.1, 53.3, 38.1. IR, ν_{max} (cm^{-1}) (CH_2Cl_2): 3736, 3159, 3123, 3104, 2224, 1702, 1602, 1572, 1503, 1485, 1469, 1447, 1407, 1358, 1292, 1237, 1214, 1183, 1151, 1126, 1071, 1016, 944, 862, 838, 824, 768, 756, 735, 692, 682, 651, 552, 491, 468, 442, 416.

Synthesis of complex 3e. Prepared according to procedure **3b** using **1e** (0.50 g, 1.32 mmol), $PdCl_2$ (0.23 g, 1.32 mmol) and K_2CO_3 (0.91 g, 6.61 mmol). Yield = 38%, 0.24 g. ^{1}H NMR (400 MHz, $CDCl_3$): δ 8.95 (t, J = 1.6 Hz, 2H, Py-H), 7.98 (d, J = 8 Hz,

Open Access Article. Published on 23 November 2021. Downloaded on 9/22/2024 3:55:22 AM. This article is licensed under a Creative Commons Attribution-NonCommercial 3.0 Unported Licence.

2H, Ar-H), 7.76 (t, $J = 1.6$ Hz, 1H, Py-H), 7.73 (d, $J = 8$ Hz, 2H, Ar-H), 7.63 (dt, $J = 7.6$ Hz, 2H, Py-H), 7.47 (m, 2H, Py-H), 7.33 (m, 2H, Ar-H), 7.01 (s, 2H, N–CHCH–N), 6.02 (s, 4H, N–CH_2). ^{13}C NMR (100 MHz, $CDCl_3$): δ 152.6, 152.3, 151.9, 151.2, 138.9, 138.8, 138.7, 138.2, 138.1, 138.0, 133.6, 133.5, 133.0, 132.9, 131.0, 130.9, 130.8, 129.1, 124.6, 124.5, 123.1, 123.0, 122.9, 117.3, 112.3, 112.2, 112.0, 52.8, 52.6, 52.4. IR, ν_{max} (cm^{-1}) (CH_2Cl_2): 3437, 3155, 3104, 2930, 2218, 1695, 1603, 1570, 1482, 1446, 1407, 1377, 1351, 1289, 1263, 1242, 1216, 1156, 1094, 1068, 1046, 1016, 966, 948, 848, 832, 795, 770, 756, 695, 684, 643, 558, 445.

Synthesis of complex 3f. Prepared according to procedure **3b** using **1f** (0.50 g, 1.98 mmol), $PdCl_2$ (0.35 g, 1.98 mmol) and K_2CO_3 (1.37 g, 9.92 mmol). Yield = 41%, 0.42 g. ^{1}H NMR (400 MHz, $CDCl_3$): δ 9.04 (t, $J = 4.8$ Hz, 2H, Py-H), 7.75 (m, 1H, Py-H), 7.91 (d, $J = 8$ Hz, 2H, Py-H), 7.36 (m, 5H, Ar-H), 6.87 (d, $J = 2$ Hz, 1H, N–CHCH–N), 6.68 (d, $J = 2$ Hz, 1H, N–CHCH–N), 5.77 (s, 2H, N–CH_2), 4.12 (s, 3H, N–CH_3). ^{13}C NMR (100 MHz, $CDCl_3$): δ 152.5, 148.4, 137.9, 135.2, 129.1, 128.9, 128.5, 124.5, 123.6, 121.3, 54.9, 38.4. IR, ν_{max} (cm^{-1}) (CH_2Cl_2): 3437, 3162, 3129, 3109, 3063, 3027, 3002, 2928, 1920, 1856, 1815, 1598, 1569, 1495, 1486, 1467, 1446, 1421, 1402, 1317, 1229, 1193, 1153, 1121, 1077, 1069, 1044, 1032, 1013, 982, 952, 835, 819, 778, 762, 732, 695, 686, 662, 641, 610, 574, 462, 445.

General procedure for the acylative Suzuki–Miyaura cross-coupling reaction of arylboronic acids with benzoyl chloride

A Radley's tube was charged with benzoyl chloride (1.2 mmol), phenylboronic acid (1.0 mmol), K_2CO_3 (1.5 mmol) and catalyst (0.1 mol%) in toluene (4 mL). The mixture was stirred to 60 °C for 4 h under an argon atmosphere. The reaction mixture was cooled to room temperature and filtered. The conversion was analyzed by ^{1}H-NMR and ^{13}C-NMR spectroscopy.

General procedure for the Suzuki–Miyaura cross-coupling reaction

A Radley's tube was charged with aryl halide (1.0 mmol), phenylboronic acid (1.0 mmol), KOH (0.5 mmol) and catalyst (0.2 mol%) in 2-propanol–H_2O mixture (2 mL, 0.5 : 1.5). The mixture was stirred to 82 °C for 30 min. under air atmosphere. The reaction mixture was cooled to room temperature and filtered. The conversion was analyzed by ^{1}H-NMR and ^{13}C-NMR spectroscopy.

Suzuki–Miyaura cross coupling products[15,20–26]

Benzophenone (Table 2, entry 1). ^{1}H NMR (400 MHz, $CDCl_3$): δ 7.81 (d, $J = 7.2$ Hz, 2H, Ar-H), 7.59 (t, $J = 7.6$ Hz, 1H, Ar-H), 7.48 (t, $J = 7.6$ Hz, 2H, Ar-H). ^{13}C NMR (100 MHz, $CDCl_3$): δ 196.7, 137.6, 132.4, 130.0, 128.3.

4-Methylbenzophenone (Table 2, entry 2). ^{1}H NMR (400 MHz, $CDCl_3$): δ 7.78 (m, 2H, Ar-H), 7.72 (d, $J = 8.4$ Hz, 2H, Ar-H), 7.55 (m, 1H, Ar-H), 7.47 (t, $J = 7.2$ Hz, 2H, Ar-H), 7.28 (d, $J = 8$ Hz, 2H, Ar-H), 2.44 (s, 3H, CH_3). ^{13}C NMR (100 MHz, $CDCl_3$): δ 196.5, 143.3, 137.9, 134.8, 132.2, 130.3, 129.9, 128.9, 128.2, 21.7.

2-Methylbenzophenone (Table 2, entry 3). ^{1}H NMR (400 MHz, $CDCl_3$): δ 8.17 (d, $J = 7.2$ Hz, 2H, Ar-H), 7.81 (d, $J = 6.8$ Hz, 1H, Ar-H), 7.67 (t, $J = 8.8$ Hz, 1H, Ar-H), 7.58 (t, $J = 7.6$ Hz, 1H, Ar-H), 7.53 (t, $J = 8$ Hz, 1H, Ar-H), 7.44 (m, 2H, Ar-H), 7.28 (m, 1H, Ar-H), 2.34 (s, 3H, CH_3). ^{13}C NMR (100 MHz, $CDCl_3$): δ 198.6, 162.8, 138.6, 136.7, 134.6, 133.2, 131.0, 130.6, 130.1, 128.9, 128.5, 125.2, 19.9.

2,4-Dimethylbenzophenone (Table 2, entry 4). ^{1}H NMR (400 MHz, $CDCl_3$): δ 8.17–8.16 (dd, $J = 6.4$ Hz, 1H, Ar-H), 7.79 (d, $J = 7.2$ Hz, 1H, Ar-H), 7.68 (t, $J = 8.8$ Hz, 1H, Ar-H), 7.55 (m, 2H, Ar-H), 7.44 (t, $J = 8$ Hz, 1H, Ar-H), 7.06 (t, $J = 8$ Hz, 1H, Ar-H), 2.38 (s, 3H, CH_3), 2.34 (s, 3H, CH_3). ^{13}C NMR (100 MHz, $CDCl_3$): δ 198.6, 140.7, 138.2, 137.3, 135.5, 133.8, 132.8, 131.9, 130.1, 129.3, 128.5, 128.3, 125.8, 21.4, 20.1.

4-Chloro-2-methylbenzophenone (Table 2, entry 5). ^{1}H NMR (400 MHz, $CDCl_3$): δ 7.78 (m, 2H, Ar-H), 7.59 (m, 1H, Ar-H), 7.46 (m, 2H, Ar-H), 7.27 (m, 3H, Ar-H), 2.32 (s, 3H, CH_3). ^{13}C NMR (100 MHz, $CDCl_3$): δ 197.5, 139.1, 137.4, 136.8, 136.1, 133.4, 131.0, 130.0, 128.6, 125.4, 19.9.

2-Fluoro, 4-methoxybenzophenone (Table 2, entry 6). ^{1}H NMR (400 MHz, $CDCl_3$): δ 7.77–7.75 (dd, $J = 6.8$ Hz, 2H, Ar-H), 7.70 (d, $J = 6.8$ Hz, 1H, Ar-H), 7.58 (m, 2H, Ar-H), 7.47 (m, 2H, Ar-H), 7.08 (t, $J = 8$ Hz, 1H, Ar-H), 2.32 (s, 3H, CH_3). ^{13}C NMR (100 MHz, $CDCl_3$): δ 195.6, 165.3, 162.7, 137.6, 133.8, 132.4, 129.9, 128.3, 125.3, 125.1, 115.0, 14.6. ^{19}F NMR (376.2 MHz, $CDCl_3$): δ −110.13 (m, F).

4-Cyanobenzophenone (Table 2, entry 7). ^{1}H NMR (400 MHz, $CDCl_3$): δ 7.87 (m, 2H, Ar-H), 7.79 (m, 4H, Ar-H), 7.65 (m, 1H, Ar-H), 7.52 (m, 2H, Ar-H). ^{13}C NMR (100 MHz, $CDCl_3$): δ 195.0, 141.2, 136.3, 133.3, 132.9, 132.2, 130.2, 130.0, 128.6, 127.9, 117.9, 115.6.

4-(Trifluoromethyl)benzophenone (Table 2, entry 8). ^{1}H NMR (400 MHz, $CDCl_3$): δ 7.90 (m, 2H, Ar-H), 7.81 (m, 2H, Ar-H), 7.76–7.75 (dd, $J = 8.8$ Hz, 2H, Ar-H), 7.63 (m, 1H, Ar-H), 7.51 (m, 2H, Ar-H). ^{13}C NMR (100 MHz, $CDCl_3$): δ 195.5, 140.7, 140.6, 136.7, 133.1, 130.1, 130.0, 128.5, 125.4, 125.3. ^{19}F NMR (376.2 MHz, $CDCl_3$): δ −63.02 (s, CF_3).

4-Chloro-2-methyl-4′-nitrobenzophenone (Table 2, entry 9). ^{1}H NMR (400 MHz, $CDCl_3$): δ 8.30 (d, $J = 6.8$ Hz, 2H, Ar-H), 7.91 (d, $J = 8.8$ Hz, 2H, Ar-H), 7.34 (s, 1H, Ar-H), 2.37 (s, 3H, CH_3). ^{13}C NMR (100 MHz, $CDCl_3$): δ 195.5, 150.3, 142.5, 139.9, 137.4, 135.2, 131.6, 130.8, 130.6, 125.7, 123.7, 20.2.

4-Trifluoromethyl-4′-nitrobenzophenone (Table 2, entry 10). ^{1}H NMR (400 MHz, $CDCl_3$): δ 8.35 (d, $J = 8.8$ Hz, 2H, Ar-H), 7.93 (d, $J = 8.8$ Hz, 2H, Ar-H), 7.87 (d, $J = 8.8$ Hz, 2H, Ar-H), 7.35 (d, $J = 8.4$ Hz, 2H, Ar-H). ^{13}C NMR (100 MHz, $CDCl_3$): δ 193.2, 152.8, 149.9, 142.3, 134.4, 132.1, 130.6, 123.7, 120.5. ^{19}F NMR (376.2 MHz, $CDCl_3$): δ −57.62 (s, CF_3).

4-Bromo-4′-nitrobenzophenone (Table 2, entry 11). ^{1}H NMR (400 MHz, $CDCl_3$): δ 8.35 (m, 2H, Ar-H), 7.93 (m, 2H, Ar-H), 7.69 (d, $J = 2.8$ Hz, 2H, Ar-H), 7.62–7.61 (dd, $J = 2.4$ Hz, 1H, Ar-H), 7.52–7.50 (dd, $J = 2.4$ Hz, 1H, Ar-H). ^{13}C NMR (100 MHz, $CDCl_3$): δ 193.7, 142.3, 134.9, 132.2, 132.0, 131.5, 130.8, 130.6, 128.8, 127.1, 123.6.

4′-Nitrobenzophenone (Table 2, entry 12). ^{1}H NMR (400 MHz, $CDCl_3$): δ 8.33 (d, $J = 8.8$ Hz, 2H, Ar-H), 7.93 (d, $J = 8.8$ Hz,

© 2021 The Author(s). Published by the Royal Society of Chemistry

Open Access Article. Published on 23 November 2021. Downloaded on 9/22/2024 3:55:22 AM. This article is licensed under a Creative Commons Attribution-NonCommercial 3.0 Unported Licence.

2H, Ar-H), 7.80 (m, 2H, Ar-H), 7.65 (m, 1H, Ar-H), 7.52 (t, J = 8 Hz, 2H, Ar-H). ^{13}C NMR (100 MHz, $CDCl_3$): δ 194.8, 149.8, 142.9, 136.3, 133.4, 130.7, 130.1, 128.7, 123.5.

Biphenyl [29] (Table 4, entry 1). ^{1}H NMR (400 MHz, $CDCl_3$): δ 7.62 (d, J = 8.4 Hz, 4H, Ar-H), 7.46 (t, J = 7.6 Hz, 4H, Ar-H), 7.37 (t, J = 8 Hz, 2H, Ar-H). ^{13}C NMR (100 MHz, $CDCl_3$): δ 141.3, 128.8, 127.3, 127.2.

4-Methylbiphenyl (Table 4, entry 2). ^{1}H NMR (400 MHz, $CDCl_3$): δ 7.63 (d, J = 8.4 Hz, 2H, Ar-H), 7.52 (d, J = 8 Hz, 2H, Ar-H), 7.47 (t, J = 7.6 Hz, 2H, Ar-H), 7.36 (m, 1H, Ar-H), 7.29 (d, J = 8 Hz, 2H, Ar-H), 2.44 (s, 3H, CH_3). ^{13}C NMR (100 MHz, $CDCl_3$): δ 141.2, 138.4, 137.0, 129.5, 128.7, 127.0, 126.9, 21.1.

4-*Tert*-butylbiphenyl (Table 4, entry 3). ^{1}H NMR (400 MHz, $CDCl_3$): δ 7.62 (d, J = 7.6 Hz, 2H, Ar-H), 7.57 (d, J = 8.4 Hz, 2H, Ar-H), 7.47 (m, 4H, Ar-H), 7.35 (t, J = 8 Hz, 1H, Ar-H), 1.39 (s, 9H, $C(CH_3)_3$). ^{13}C NMR (100 MHz, $CDCl_3$): δ 150.3, 141.1, 138.4, 128.7, 127.1, 127.0, 126.8, 125.7, 34.9, 31.4.

4-Hydroxybiphenyl (Table 4, entry 4). ^{1}H NMR (400 MHz, DMSO-d_6): δ 9.53 (s, 1H, OH), 7. 54 (d, J = 8.4 Hz, 2H, Ar-H), 7.46 (d, J = 8.4 Hz, 2H, Ar-H), 7.38 (t, J = 7.2 Hz, 1H, Ar-H), 6.84 (d, J = 8.8 Hz, 2H, Ar-H). ^{13}C NMR (100 MHz, DMSO-d_6): δ 157.9, 140.7, 131.4, 129.2, 128.2, 126.8, 126.4, 116.2.

4-Cyanobiphenyl (Table 4, entry 5). ^{1}H NMR (400 MHz, $CDCl_3$): δ 7.69 (m, 4H, Ar-H), 7.59 (m, 2H, Ar-H), 7.49 (m, 2H, Ar-H), 7.44 (m, 1H, Ar-H). ^{13}C NMR (100 MHz, $CDCl_3$): δ 145.6, 139.1, 132.9, 129.1, 128.7, 127.7, 127.2, 118.9, 110.9.

4-Fluorobiphenyl (Table 4, entry 6). ^{1}H NMR (400 MHz, $CDCl_3$): δ 7.57 (m, 4H, Ar-H), 7. 46 (t, J = 8 Hz, 2H, Ar-H), 7. 37 (t, J = 8.8 Hz, 1H, Ar-H), 7.15 (m, 2H, Ar-H). ^{13}C NMR (100 MHz, $CDCl_3$): δ 163.7, 161.3, 140.3, 137.4, 128.8, 127.7, 127.6, 127.3, 127.0, 115.7, 115.5. ^{19}F NMR (376.2 MHz, $CDCl_3$): δ −115.82 (m, F).

4-(Trifluoromethyl)biphenyl (Table 4, entry 7). ^{1}H NMR (400 MHz, $CDCl_3$): δ 7.71 (s, 4H, Ar-H), 7.62 (d, J = 7.2 Hz, 2H, Ar-H), 7.49 (t, J = 6.8 Hz, 2H, Ar-H), 7.43 (d, J = 7.6 Hz, 1H, Ar-H). ^{13}C NMR (100 MHz, $CDCl_3$): δ 139.8, 128.9, 128.2, 127.4, 127.3, 125.8, 125.7, 125. 7, 125.6. ^{19}F NMR (376.2 MHz, $CDCl_3$): δ −62.40 (s, CF_3).

4-(Trifluoromethoxy)biphenyl (Table 4, entry 8). ^{1}H NMR (400 MHz, $CDCl_3$): δ 7.58 (m, 4H, Ar-H), 7. 46 (t, J = 7.2 Hz, 2H, Ar-H), 7.38 (t, J = 8 Hz, 1H, Ar-H), 7.28 (t, J = 8.8 Hz, 2H, Ar-H). ^{13}C NMR (100 MHz, $CDCl_3$): δ 148.7, 139.9, 139.8, 128.9, 128.4, 127.7, 127.1, 121.8, 121.2, 119.3. ^{19}F NMR (376.2 MHz, $CDCl_3$): δ −57.83 (s, OCF_3).

2-Hydroxybiphenyl (Table 4, entry 9). ^{1}H NMR (400 MHz, $CDCl_3$): δ 7.50 (m, 4H, Ar-H), 7.41 (m, 1H, Ar-H), 7.28 (m, 2H, Ar-H), 7.01 (t, J = 7.6 Hz, 2H, Ar-H), 5.21 (s, 1H, OH). ^{13}C NMR (100 MHz, $CDCl_3$): δ 152.4, 137.1, 130.3, 129.3, 129.2, 129.1, 128.1, 127.9, 120.9, 115.8.

2-Methylbiphenyl (Table 4, entry 10). ^{1}H NMR (400 MHz, $CDCl_3$): δ 7.43 (m, 2H, Ar-H), 7.53 (m, 3H, Ar-H), 7.28 (m, 2H, Ar-H), 7.25 (m, 2H, Ar-H), 2.29 (s, 3H, CH_3). ^{13}C NMR (100 MHz, $CDCl_3$): δ 141.9, 141.9, 135.3, 130.3, 129.8, 129.2, 128.1, 127.2, 126.7, 125.7, 20.5.

2-(Trifluoromethyl)biphenyl (Table 4, entry 11). ^{1}H NMR (400 MHz, $CDCl_3$): δ 7.75 (d, J = 7.2 Hz, 1H, Ar-H), 7.59 (m, 1H, Ar-H), 7.47 (t, J = 8 Hz, 1H, Ar-H), 7.41 (d, J = 5.2 Hz, 3H, Ar-H), 7.34 (m, 3H, Ar-H). ^{13}C NMR (100 MHz, $CDCl_3$): δ 139.8, 132.0, 131.2, 128.9, 128.7, 127.7, 127.9, 127.3, 127.2, 126.0, 125.9. ^{19}F NMR (376.2 MHz, $CDCl_3$): δ −56.86 (s, CF_3).

4-Chloro-2-methylbiphenyl (Table 4, entry 12). ^{1}H NMR (400 MHz, $CDCl_3$): δ 7.42 (t, J = 7.2 Hz, 2H, Ar-H), 7.36 (m, 1H, Ar-H), 7.29 (d, J = 8 Hz, 3H, Ar-H), 7.23 (d, J = 7.6 Hz, 1H, Ar-H), 7.16 (d, J = 8.4 Hz, 1H, Ar-H), 2.26 (s, 3H, CH_3). ^{13}C NMR (100 MHz, $CDCl_3$): δ 140.8, 140.4, 137.3, 132.9, 131.0, 130.1, 129.1, 128.2, 127.1, 125.9, 20.4.

2,4-Methylbiphenyl (Table 4, entry 13). ^{1}H NMR (400 MHz, $CDCl_3$): δ 7.42 (m, 2H, Ar-H), 7. 35 (t, J = 5.6 Hz, 3H, Ar-H), 7.12 (m, 3H, Ar-H), 2.39 (s, 3H, CH_3), 2.27 (s, 3H, CH_3). ^{13}C NMR (100 MHz, $CDCl_3$): δ 141.9, 139.1, 136.9, 135.1, 131.1, 129.8, 129.3, 128.0, 126.6, 126.5, 21.1, 20.4.

4-Fluoro-3-methylbiphenyl (Table 4, entry 14). ^{1}H NMR (400 MHz, $CDCl_3$): δ 7.55 (d, J = 8.4 Hz, 2H, Ar-H), 7.43 (t, J = 7.6 Hz, 3H, Ar-H), 7.37 (m, 3H, Ar-H), 7.07 (t, J = 8.8 Hz, 1H, Ar-H), 2.35 (s, 3H, CH_3). ^{13}C NMR (100 MHz, $CDCl_3$): δ 162.3, 159.8, 140.5, 130.3, 130.2, 128.8, 127.2, 127.1, 127.0, 126.0, 125.9, 125.1, 124.9, 115.1, 14.7, 14.7. ^{19}F NMR (376.2 MHz, $CDCl_3$): δ −120.18 (m, F).

2-Fluoro-4-methylbiphenyl (Table 4, entry 15). ^{1}H NMR (400 MHz, $CDCl_3$): δ 7.55 (d, J = 8.4 Hz, 2H, Ar-H), 7.45 (t, J = 7.6 Hz, 3H, Ar-H), 7.39 (m, 2H, Ar-H), 7.08 (t, J = 8.8 Hz, 1H, Ar-H), 2.36 (s, 3H, CH_3). ^{13}C NMR (100 MHz, $CDCl_3$): δ 130.3, 130.2, 128.7, 127.1, 126.9, 125.9, 125.8, 115.3, 115.1, 14.7. ^{19}F NMR (376.2 MHz, $CDCl_3$): δ −120.17 (m, F).

4-Methyl-3-nitrobiphenyl (Table 4, entry 16). ^{1}H NMR (400 MHz, $CDCl_3$): δ 8.21 (d, J = 1.6 Hz, 1H, Ar-H), 7.73 (d, J = 8 Hz, 1H, Ar-H), 7.60 (d, J = 8 Hz, 2H, Ar-H), 7.48 (t, J = 7.2 Hz, 2H, Ar-H), 7.41 (m, 2H, Ar-H), 2.64 (s, 3H, CH_3). ^{13}C NMR (100 MHz, $CDCl_3$): δ 140.2, 138.4, 133.6, 133.2, 132.2, 131.3, 129.1, 128.3, 126.9, 122.9, 20.1.

4′-Methylbiphenyl (Table 4, entry 17). ^{1}H NMR (400 MHz, $CDCl_3$): δ 7.61 (d, J = 8 Hz, 2H, Ar-H), 7.53 (d, J = 8 Hz, 2H, Ar-H), 7.45 (t, J = 7.6 Hz, 2H, Ar-H), 7.35 (t, J = 7.6 Hz, 1H, Ar-H), 7.28 (d, J = 8 Hz, 2H, Ar-H), 2.42 (s, 3H, CH_3). ^{13}C NMR (100 MHz, $CDCl_3$): δ 141.2, 138.4, 137.0, 129.5, 128.7, 127.0, 127.0, 21.1.

4′-Methoxybiphenyl (Table 4, entry 18). ^{1}H NMR (400 MHz, $CDCl_3$): δ 7.56 (m, 4H, Ar-H), 7.43 (t, J = 7.6 Hz, 2H, Ar-H), 7.32 (t, J = 7.6 Hz, 1H, Ar-H), 7.00 (m, 2H, Ar-H), 3.87 (s, 3H, CH_3). ^{13}C NMR (100 MHz, $CDCl_3$): δ 159.2, 140.9, 133.8, 128.8, 128.2, 126.8, 126.7, 114.2, 55.4.

Conflicts of interest

There are no conflicts to declare.

Acknowledgements

Financial support from Ege University (Project FYL-2018-20197) is gratefully acknowledged. The authors acknowledge Dokuz Eylul University for using of the Rigaku Oxford Xcalibur Eos Diffractometer (purchased under University Research Grant No. 2010.KB.FEN.13). Dr Senthil Rethinam acknowledges the funding support granted by the 2232-International Fellowship for Outstanding Researcher Program of TUBITAK (Project No: 118C350).

Open Access Article. Published on 23 November 2021. Downloaded on 9/22/2024 3:55:22 AM. This article is licensed under a Creative Commons Attribution-NonCommercial 3.0 Unported Licence.

Notes and references

1 K. C. Nicolaou, P. G. Bulger and D. Sarlah, *Angew. Chem., Int. Ed.*, 2005, **44**, 4442–4489.
2 L. Yin and J. Liebscher, *Chem. Rev.*, 2007, **107**, 133–137.
3 (*a*) B. M. Baughman, E. Stennett, R. E. Lipner, A. C. Rudawsky and S. J. Schidtke, *J. Phys. Chem. A*, 2009, **113**, 8011; (*b*) C. Torborg and M. Beller, *Adv. Synth. Catal.*, 2009, **351**, 3027–3043; (*c*) C. M. So and F. Y. Kwong, *Chem. Soc. Rev.*, 2011, **40**, 4963; (*d*) I. P. Beletskaya, F. Alonso and V. Tyurin, *Coord. Chem. Rev.*, 2019, **385**, 137–173.
4 M. Blangetti, H. Rosso, C. Prandi, A. Deagostino and P. Venturello, *Molecules*, 2013, **18**, 1188.
5 J. Buchspies and M. Szostak, *Catalysts*, 2019, **9**, 53.
6 (*a*) C. Fliedel, A. Labande, E. Manoury and R. Poli, *Coord. Chem. Rev.*, 2019, **394**, 65–103; (*b*) G. C. Fortman and S. P. Nolan, *Chem. Soc. Rev.*, 2011, **40**, 5151–5516.
7 (*a*) C. Fliedel, A. Ghisolfi and P. Braunstein, *Chem. Rev.*, 2016, **116**(16), 9237–9304; (*b*) N. T. S. Phan, M. V. D. Sluys and C. W. Jones, *Adv. Synth. Catal.*, 2006, **348**(6), 609–679; (*c*) Y. C. Wong, K. Parthasarathy and C. H. Cheng, *Org. Lett.*, 2010, **12**, 1736.
8 (*a*) H. W. Wanzlick and H. J. Schonherr, *Angew. Chem., Int. Ed. Engl.*, 1968, **7**, 141–143; (*b*) A. J. Arduengo, R. L. Harlow and M. Kline, *J. Am. Chem. Soc.*, 1991, **113**, 361–363.
9 H. V. Huynh, *The Organometallic Chemistry of N-Heterocyclic Carbenes*, John Wiley & Sons, Ltd, Chichester, UK, 2017.
10 A. Rühling, K. Schaepe, L. Rakers, B. Vonhören, P. Tegeder, B. J. Ravoo and F. Glorius, *Angew. Chem., Int. Ed.*, 2016, **55**, 5856–5860.
11 L. Jiang, F. Shan, Z. Li and D. Zhao, *Molecules*, 2012, **17**, 12121–12139.
12 (*a*) N. A. Bumagin and D. N. Korolev, *Tetrahedron Lett.*, 1999, **40**, 3057–3060; (*b*) M. Haddach and J. R. McCarthy, *Tetrahedron Lett.*, 1999, **40**, 3109–3112; (*c*) L. Zhang, J. Wu, L. Shi, C. Xia and F. Li, *Tetrahedron Lett.*, 2011, **52**, 3897–3901; (*d*) M. Mondal and U. Bora, *Appl. Organomet. Chem.*, 2018, **28**, 354–358; (*e*) H. Solařová, I. Císařová and P. Štěpnička, *Organometallics*, 2014, **33**, 4131–4147; (*f*) M. Semler and P. Štěpnička, *Catal. Today*, 2015, **243**, 128–133; (*g*) F. Rafiee and A. R. Hajipour, *Appl. Organomet. Chem.*, 2015, **29**, 181–184; (*h*) M. Mondal and U. Bora, *New J. Chem.*, 2016, **40**, 3119–3123; (*i*) B. Movassagh, F. Hajizadeh and E. Mohammadi, *Appl. Organomet. Chem.*, 2018, **32**, e3982.
13 (*a*) J.-Y. Chen, S.-C. Chen, Y.-J. Tang, C.-Y. Mou and F.-Y. Tsai, *J. Mol. Catal. A: Chem.*, 2009, **88**, 307; (*b*) D. J. Nelson and S. P. Nolan, *Chem. Soc. Rev.*, 2013, **42**, 6723; (*c*) H. Türkmen and B. Çetinkaya, *J. Organomet. Chem.*, 2006, **691**, 3749–3759; (*d*) E. Gacal, S. Denizaltı, A. Kınal, A. G. Gökçe and H. Türkmen, *Tetrahedron*, 2018, **74**, 6829–6838; (*e*) H. Türkmen, R. Can and B. Çetinkaya, *Dalton Trans.*, 2009, 7039–7044.
14 H. M. J. Wang and I. J. B. Lin, *Organometallics*, 1998, **17**, 972–975.
15 M. Sevim, S. B. Kavukcu, A. Kınal, O. Şahin and H. Türkmen, *Dalton Trans.*, 2020, **49**, 16903–16915.
16 C. F. R. A. C. Lima, A. S. M. C. Rodrigues, V. L. M. Silva, A. M. S. Silva and L. M. N. B. F. Santos, *ChemCatChem*, 2014, **6**(5), 1291–1302.
17 CrysAlisPro Software System, Rigaku Oxford Diffraction, 2019.
18 G. M. Sheldrick, *Acta Crystallogr., Sect. A: Found. Adv.*, 2015, **71**, 3–8.
19 O. V. Dolomanov, L. J. Bourhis, R. J. Gildea, J. A. K. Howard and H. Puschmann, *J. Appl. Crystallogr.*, 2009, **42**, 339–341.
20 Y. C. Wong, K. Parthasarathy and C. H. Cheng, *Org. Lett.*, 2010, **12**, 1736.
21 J.-Y. Chen, S.-C. Chen, Y.-J. Tang, C.-Y. Mou and F.-Y. Tsai, *J. Mol. Catal. A: Chem.*, 2009, **88**, 307.
22 M. Li, C. Wang and H. Ge, *Org. Lett.*, 2011, **13**, 2062.
23 D. Xing, B. Guan, G. Cai, Z. Fang, L. Yang and Z. Shi, *Org. Lett.*, 2006, **8**, 693.
24 W. J. Zhou, K. H. Wang and J. X. Wang, *J. Org. Chem.*, 2009, **74**, 5599.
25 L. Liu, Y. Zhang and B. Xin, *J. Org. Chem.*, 2006, **71**, 3994.
26 L. Liu, Y. Zhang and Y. Wang, *J. Org. Chem.*, 2005, **70**, 6122.
27 (*a*) S. Çakır, G. Türkmen and H. Türkmen, *Appl. Organomet. Chem.*, 2018, **32**, e3969; (*b*) S. Çakır and H. Türkmen, *Appl. Organomet. Chem.*, 2020, **34**, e5499.
28 Z. Fei, D. Zhao, D. Pieraccini, W. H. Ang, T. J. Geldbach, R. Scopelliti, C. Chiappe and P. J. Dyson, *Organometallics*, 2007, **26**, 1588–1598.
29 (*a*) F. E. Hahn and M. C. Jahnke, *Angew. Chem., Int. Ed.*, 2008, **47**, 3122–3172; (*b*) S. Díez-González, N. Marion and S. P. Nolan, *Chem. Rev.*, 2009, **109**, 3612–3676; (*c*) T. Dröge and F. Glorius, *Angew. Chem., Int. Ed.*, 2010, **49**, 6940–6952; (*d*) Z. Jin, L.-L. Qiu, Y.-Q. Li, H.-B. Song and J.-X. Fang, *Organometallics*, 2010, **29**, 6578–6586; (*e*) G. C. Fortman and S. P. Nolan, *Chem. Soc. Rev.*, 2011, **40**, 5151–5169.
30 (*a*) R. A. Kelly III, H. Clavier, S. Giudice, N. M. Scott, E. D. Stevens, J. Bordner, I. Samardjiev, C. D. Hoff, L. Cavallo and S. P. Nolan, *Organometallics*, 2008, **27**, 202–210; (*b*) D. J. Nelson and S. P. Nolan, *Chem. Soc. Rev.*, 2013, **42**, 6723–6753.
31 (*a*) M. G. Organ, M. AbdelHadi, S. Avola, I. Dubovyk, N. Hadei, E. A. B. Kantchev, C. J. O'Brien, M. Sayah and C. Valente, *Chem.–Eur. J.*, 2008, **14**, 2443–2452; (*b*) L. Xu and Y. Shi, *J. Org. Chem.*, 2008, **73**, 749–751; (*c*) K. H. Hoi, S. Çalimsiz, R. D. J. Froese, A. C. Hopkinson and M. G. Organ, *Chem.–Eur. J.*, 2011, **17**, 3086–3090; (*d*) C. Valente, S. Çalimsiz, K. H. Hoi, D. Mallik, M. Sayah and M. G. Organ, *Angew. Chem., Int. Ed.*, 2012, **51**, 3314–3332; (*e*) A. Chartoire, X. Frogneux, A. Boreux, A. M. Z. Slawin and S. P. Nolan, *Organometallics*, 2012, **31**, 6947–6951; (*f*) J.-S. Ouyang, S. Liu, B. Pen, Y. Zhang, H. Liang, B. Chen, X. He, W. T. K. Chan, A. S. C. Chan, T.-Y. Sun, Y.-D. Wu and L. Qiu, *ACS Catal.*, 2021, **11**, 9252–9261.
32 (*a*) C. Yang, L. Zhang, C. Lu, S. Zhou, X. Li, Y. Li, Y. Yang, Y. Li, Z. Liu, J. Yang, K. N. Houk, F. Mo and X. Guo, *Nat. Nanotechnol.*, 2021, **16**, 1214–1223; (*b*) N. Marion and S. P. Nolan, *Acc. Chem. Res.*, 2008, **41**, 1440–1449.
33 G. Li, P. Lei, M. Szostak, E. Casals-Cruañas, A. Poater, L. Cavallo and S. P. Nolan, *ChemCatChem*, 2018, **10**, 3096–3106.

© 2021 The Author(s). Published by the Royal Society of Chemistry

Open Access Article. Published on 23 November 2021. Downloaded on 9/22/2024 3:55:22 AM.
This article is licensed under a Creative Commons Attribution-NonCommercial 3.0 Unported Licence.

34 C. F. R. A. C. Lima, A. S. M. C. Rodrigues, V. L. M. Silva, A. M. S. Silva and L. M. N. B. F. Santos, *ChemCatChem*, 2014, **6**, 1291–1302.

35 (*a*) S. Yang, T. Zhou, A. Poater, L. Cavallo, S. P. Nolan and M. Szostak, *Catal. Sci. Technol.*, 2021, **11**, 3189–3197; (*b*) G. Li, P. Lei, M. Szostak, E. Casals-Cruañas, A. Poater, L. Cavallo and S. P. Nolan, *ChemCatChem*, 2018, **10**, 3096–3106; (*c*) G. M. Meconi, S. V. C. Vummaleti, J. A. Luque-Urrutia, P. Belanzoni, S. P. Nolan, H. Jacobsen, L. Cavallo, M. Solà and A. Poater, *Organometallics*, 2017, **36**, 2088–2095.

36 R. Gajda, A. Poater, A. Brotons-Rufes, S. Planer, K. Woźniak, K. Grela and A. Kajetanowicz, *Arkivoc*, 2021, 138–156.

37 (*a*) M. G. Organ, G. A. Chass, D.-C. Fang, A. C. Hopkinson and C. Valente, *Synthesis*, 2008, **2008**, 2776–2797; (*b*) C. Valente, M. Pompeo, M. Sayah and M. G. Organ, *Org. Process Res. Dev.*, 2014, **18**, 180–190; (*c*) R. D. J. Froese, C. Lombardi, M. Pompeo, R. P. Rucker and M. G. Organ, *Acc. Chem. Res.*, 2017, **50**, 2244–2253.

© 2021 The Author(s). Published by the Royal Society of Chemistry